

# Primordial Black Holes Place the Universe in Stasis

Keith R. Dienes,<sup>1,2,\*</sup> Lucien Heurtier,<sup>3,†</sup> Fei Huang,<sup>4,5,6,‡</sup> Doojin Kim,<sup>7,§</sup>  
Tim M.P. Tait,<sup>5,¶</sup> Brooks Thomas<sup>8,\*\*</sup>

<sup>1</sup>*Department of Physics, University of Arizona, Tucson, AZ 85721 USA*

<sup>2</sup>*Department of Physics, University of Maryland, College Park, MD 20742 USA*

<sup>3</sup>*IPPP, Durham University, Durham, DH1 3LE, United Kingdom*

<sup>4</sup>*CAS Key Laboratory of Theoretical Physics, Institute of Theoretical Physics,  
Chinese Academy of Sciences, Beijing 100190, China*

<sup>5</sup>*Department of Physics and Astronomy, University of California, Irvine, CA 92697 USA*

<sup>6</sup>*Department of Particle Physics and Astrophysics,  
Weizmann Institute of Science, Rehovot 7610001, Israel*

<sup>7</sup>*Mitchell Institute for Fundamental Physics and Astronomy,*

*Department of Physics and Astronomy, Texas A&M University, College Station, TX 77843 USA*

<sup>8</sup>*Department of Physics, Lafayette College, Easton, PA 18042 USA*

A variety of scenarios for early-universe cosmology give rise to a population of primordial black holes (PBHs) with a broad spectrum of masses. The evaporation of PBHs in such scenarios has the potential to place the universe into an extended period of “stasis” during which the abundances of matter and radiation remain absolutely constant despite cosmological expansion. This surprising phenomenon can give rise to new possibilities for early-universe dynamics and lead to distinctive signatures of the evaporation of such PBHs. In this paper, we discuss how this stasis epoch arises and explore a number of its phenomenological consequences, including implications for inflationary observables, the stochastic gravitational-wave background, baryogenesis, and the production of dark matter and dark radiation.

## CONTENTS

## References

22

|  |    |
|--|----|
| I. Introduction  | 1  |
| II. The Emergence of A Stasis Epoch                      | 2  |
| A. PBH Formation   | 2  |
| B. PBH Evaporation                                       | 3  |
| C. Evolution of the Energy Density                       | 4  |
| D. Cosmological Dynamics and the Emergence of Stasis     | 4  |
| III. Stasis in the Early Universe: Stasis is Not Eternal | 7  |
| IV. Phenomenological Implications of PBH-Induced Stasis  | 8  |
| A. Cosmic Expansion History                              | 9  |
| B. Inflation   | 10 |
| C. Gravitational Waves                                   | 11 |
| D. Dark Radiation  | 17 |
| E. Dark Matter   | 18 |
| F. Baryogenesis  | 20 |
| V. Conclusions   | 20 |
| Acknowledgements   | 21 |

## I. INTRODUCTION

In a broad class of inflationary scenarios, a population of black holes (BHs) is generated shortly after inflation as a consequence of the gravitational collapse of primordial density fluctuations. Such primordial black holes (PBHs) have received a significant amount of recent attention, in part because they can potentially provide a solution to the dark-matter problem. Indeed, while black holes evaporate over time as a consequence of Hawking radiation [1, 2], PBHs with masses  $M \gtrsim 10^{15}$  g would nevertheless have lifetimes longer than the age of the universe. Indeed, a population of PBHs with masses within the range  $10^{17}$  g  $\lesssim M \lesssim 10^{23}$  g can potentially account for the entirety of the present-day dark-matter abundance, even when the spectrum of PBHs is approximately monochromatic (for reviews, see, *e.g.*, Refs. [3–6]). PBHs with lower masses can also have implications for cosmology. Indeed, PBHs with masses in the range  $10^9$  g  $\lesssim M \lesssim 10^{14}$  g evaporate at a significant rate during or after Big-Bang nucleosynthesis (BBN), generating energetic particles which can modify the primordial abundances of light nuclei. As a result, the abundance of PBHs with masses in this range is tightly constrained [4, 7, 8].

By contrast, PBHs with masses  $M \lesssim 10^9$  g evaporate completely prior to the BBN epoch and are therefore essentially unconstrained by these considerations. For this reason, far less attention has been focused on PBHs within this mass range. Nevertheless, such light PBHs

\* Email address: [dienes@arizona.edu](mailto:dienes@arizona.edu)

† Email address: [lucien.heurtier@durham.ac.uk](mailto:lucien.heurtier@durham.ac.uk)

‡ Email address: [fei.huang@weizmann.ac.il](mailto:fei.huang@weizmann.ac.il)

§ Email address: [doojin.kim@tamu.edu](mailto:doojin.kim@tamu.edu)

¶ Email address: [ttait@uci.edu](mailto:ttait@uci.edu)

\*\* Email address: [thomasbd@lafayette.edu](mailto:thomasbd@lafayette.edu)

can potentially have an impact on early-universe cosmology. For example, their evaporation can serve as a source for dark matter or dark radiation [9–31]. Such PBHs can also trigger baryogenesis [32–36] or lead to an epoch of early matter domination [37].

In this paper, we point out that a population of PBHs with masses in this range can also have another important impact on early-universe cosmology. In particular, as first noted in Ref. [38], such a population of PBHs can give rise to an extended period during which the abundances of PBHs and radiation can remain relatively constant. Indeed, this is an example of *cosmic stasis* [39], a general phenomenon wherein multiple cosmological components with different equations of state — in this case, matter in the form of black holes and the radiation generated by their evaporation — have abundances which remain constant despite cosmological expansion. Since the energy density of radiation dilutes faster as a result of cosmic expansion than does that of matter, the abundance of matter typically increases over time, while the abundance of radiation decreases. Thus, in order for a stasis epoch involving these two cosmological components to arise, a mechanism must exist which counteracts this tendency by gradually transferring energy density from matter to radiation over an extended period. In Ref. [39], it was shown that particle decay constitutes such a mechanism in the case in which the matter sector consists of a tower of unstable particles with a broad spectrum of lifetimes and individual abundances. However, as shown in Ref. [38] and as we shall demonstrate here, Hawking radiation likewise provides such a mechanism in the case in which the matter sector comprises a population of PBHs.

This paper is devoted to a study of PBH-induced stasis and its phenomenological consequences for the early universe. In Sect. II, we begin by reviewing the critical ingredients which are needed for our subsequent analysis. In particular, we consider the processes through which a population of PBHs can arise in the early universe and discuss the resulting PBH mass spectra. We also review the dynamics of PBH evaporation and assess the impact of this dynamics on the overall energy density of this population. We then review how this dynamics can give rise to a period of cosmic stasis — one which is a global attractor within cosmologies of this sort. Having thus set the stage for our work, we then proceed to the main purpose of this paper, namely to study some of the phenomenological implications of a period of cosmic stasis. We begin in Sect. III by demonstrating that cosmic stasis not only has a beginning *but also an end*, so that the universe can not only enter into stasis in a natural way but also exit from it equally naturally. This property allows stasis to be the underpinning of a true cosmological *epoch* from which the universe may subsequently transition into an epoch of another type, thereby allowing it to be “spliced” into more traditional cosmological timelines. In Sect. IV, we then proceed to consider various phenomenological implications of a PBH-induced period of stasis. In particular, in Sect. IV A we consider the effects

of a stasis epoch on the cosmic expansion history, while in Sect. IV B we consider the effects of such an epoch on inflationary observables. In Sect. IV C we consider the implications for gravitational waves. In Sects. IV D and IV E, we consider the effects that a PBH-induced stasis epoch can potentially have on dark-radiation and dark-matter production, respectively. In Sect. IV F we consider the implications of such an epoch for baryogenesis. Finally, in Sect. V we conclude with a summary of our main results and highlight possible directions for future work.

## II. THE EMERGENCE OF A STASIS EPOCH

We begin by reviewing the physics that will be needed for our subsequent work. This includes the dynamics of PBH formation and evaporation, and the manner in which these features can give rise to cosmic stasis.

### A. PBH Formation

Quantum fluctuations during cosmic inflation give rise to a spectrum of primordial density fluctuations. After inflation ends, the size of a causally connected region grows as the universe expands, as does the range of gravitational interactions. More specifically, the comoving radius of such a region is given by the comoving Hubble horizon  $(aH)^{-1}$ , where  $a$  is the scale factor and  $H \equiv \dot{a}/a$  is the Hubble parameter. Primordial density fluctuations with a given comoving wavenumber  $k$  remain frozen until this comoving radius becomes comparable to  $2\pi/k$  and gravity comes into play. Any fluctuation sufficiently overdense that its radius lies below its Schwarzschild radius is expected to collapse and form a black hole. The characteristic initial mass  $M_i$  of a black hole formed in this way is (for reviews, see, *e.g.*, Ref. [40])

$$M_i = \frac{4}{3}\pi\gamma\rho\left(\frac{1}{H}\right)^3 = \frac{\gamma M_P^2}{2H}, \quad (2.1)$$

where  $\gamma$  is an  $\mathcal{O}(1)$  proportionality factor, where  $\rho$  is the average energy density of the universe at the time the fluctuation enters the horizon, and where  $M_P = G^{-1/2}$  is the Planck mass, which we define in the usual way in terms of the gravitational constant  $G$ .

As the universe expands, density fluctuations with increasingly long comoving wavelengths enter the horizon and form PBHs with different masses. The mass spectrum of these PBHs — *i.e.*, the number density  $f_{\text{BH}}(M, t)$  of PBHs per unit mass — can therefore be viewed as resulting from the interplay between two factors. The first of these is the power spectrum of primordial density perturbations present in the early universe. The second is the equation-of-state parameter of the universe  $w_c$  during the period when these perturbations collapse. We note that contributions to  $f_{\text{BH}}(M, t)$  can also be generated through other mechanisms at later times as well

(for a review, see, *e.g.*, Ref. [41]). However, we shall not consider such additional contributions in this paper.

Different scenarios for PBH production in the early universe give rise to different forms for  $f_{\text{BH}}(M, t)$ . Examples of such production scenarios include the collapse of Gaussian primordial inhomogeneities [42], inflation-induced power spectra [43–55], the collapse of density perturbations during the QCD phase transition [56–59], bubble collisions [56, 60–70], or the collapse of domain walls [67–73] and cosmic loops [74–79]. Interestingly, light PBHs can also be produced by the resonant amplification of scalar perturbations shortly after the end of cosmic inflation [80, 81]. Some of these BH-production scenarios give rise to a sharply-peaked, nearly monochromatic PBH mass spectrum. By contrast, others give rise to a spectrum which is well-modeled by a power law over a broad range of masses.

In what follows, we consider PBH spectra of this latter sort. In particular, we shall focus on a broad class of PBH mass spectra for which the initial number density  $f_{\text{BH}}(M_i, t_i)$  of PBHs per unit mass  $M_i$  at the initial time  $t_i$  at which the spectrum has effectively been established takes the form

$$f_{\text{BH}}(M_i, t_i) = \begin{cases} CM_i^{\alpha-1} & \text{for } M_{\text{min}} \leq M_i \leq M_{\text{max}} \\ 0 & \text{otherwise} \end{cases} \quad (2.2)$$

for some minimum and maximum PBH masses  $M_{\text{min}}$  and  $M_{\text{max}}$ , where  $\alpha$  is a power-law exponent and where  $C$  is an overall normalization coefficient. The corresponding energy density of PBHs per unit mass is therefore given by  $CM_i^\alpha$ .

PBH spectra of the form given in Eq. (2.2) arise naturally, for example, in scenarios in which the PBHs form via the collapse of a scale-invariant power spectrum [42, 82–85]. In scenarios of this sort, the power-law exponent  $\alpha$  is related to the value of the equation-of-state parameter  $w_c$  for the universe as a whole during the epoch immediately following inflation, during which primordial density perturbations collapse to form PBHs. In particular, one finds that

$$\alpha \equiv -\frac{3w_c + 1}{w_c + 1}. \quad (2.3)$$

Since the collapse of PBHs occurs after (rather than during) inflation, the physically motivated range for  $w_c$  is  $-1/3 < w_c \leq 1$ . Such values correspond to values of the scaling exponent

$$-2 \leq \alpha < 0. \quad (2.4)$$

Phenomenological considerations likewise place constraints on the values of  $M_{\text{min}}$  and  $M_{\text{max}}$ , although these constraints are considerably more model-dependent than those on  $\alpha$ . As discussed in the Introduction, BBN constraints on the production of energetic particles from black-hole evaporation place stringent bounds on  $f_{\text{BH}}(M_i, t_i)$ . However, PBHs with initial masses  $M_i \lesssim$

$10^9$  g evaporate before the BBN epoch begins and consequently evade these constraints [4, 7, 8]. Of course, BBN constraints on the continuous injection of energy density over an extended period depend on both on the overall energy density injected and on the time-dependent manner in which that injection occurs [86]. Since the energy density of PBHs per unit mass falls rapidly with  $M_i$  for values of  $\alpha$  at the lower end of the allowed range in Eq. (2.4), some fraction of the PBH population may evaporate after the onset of the BBN epoch without running afoul of these constraints. However, in what follows, we adopt a conservative approach and focus on the regime in which  $M_{\text{max}} \lesssim 10^9$  g.

A lower bound on  $M_{\text{min}}$  arises from CMB data, which place an upper bound  $H_* < 2.5 \times 10^{-5} M_P$  on the Hubble parameter during inflation [87]. This in turn translates into a lower bound on  $M_{\text{min}}$ . The precise value of this bound depends on the details of both the inflationary model and the mechanics of gravitational collapse. For concreteness, we take the bound  $M_{\text{min}} \gtrsim 0.1$  g [4] obtained for the case of slow-roll inflation as a rough benchmark. We emphasize, however, that bounds of this sort apply only in situations in which the population of PBHs is generated entirely from primordial perturbations which collapse upon re-entering the horizon after inflation. Additional mechanisms for PBH production which involve the gravitational collapse of overdense regions with comoving wavelengths well below  $(aH)^{-1}$  can result in PBHs with far lower masses.

Thus, in summary, we shall primarily focus on PBH mass spectra wherein  $\alpha$  falls within the range specified in Eq. (2.4) and wherein

$$0.1 \text{ g} \lesssim M_{\text{min}} < M_{\text{max}} \lesssim 10^9 \text{ g} \quad (2.5)$$

in what follows.

## B. PBH Evaporation

A Schwarzschild black hole of mass  $M$  evaporates by emitting a thermal spectrum of particles at the Hawking temperature [1, 2]

$$T_{\text{BH}} = \frac{1}{8\pi GM} \sim 1.06 \text{ GeV} \left( \frac{10^{13} \text{ g}}{M} \right). \quad (2.6)$$

The efficiency of the evaporation process depends both on  $T_{\text{BH}}$  and on the mass spectrum and quantum numbers of the particles that can be produced. When one accounts for all the corresponding graybody factors, one finds that the rate of change of  $M$  due to evaporation is [88, 89]

$$\frac{dM}{dt} \equiv -\varepsilon(M) \frac{M_P^4}{M^2}, \quad (2.7)$$

where the function  $\varepsilon(M)$  encodes how this rate varies with the BH mass and temperature.

A detailed description of how this function is computed can be found in Ref. [20] and references therein. As discussed in the Introduction, PBHs which evaporate before BBN — and which therefore evade current observational constraints — have masses  $M \lesssim 10^9$  g [4, 7, 8]. The corresponding Hawking temperatures  $T_{\text{BH}} \gtrsim 10^4$  GeV for PBHs in this mass range are sufficiently high that the average momentum of any Standard-Model particles produced as Hawking radiation is  $\langle p \rangle \sim T_{\text{BH}}$ . As a result, provided that any additional particle species that might happen to be present in the theory likewise have masses that lie well below this value of  $T_{\text{BH}}$ , one finds that  $\varepsilon(M)$  can be approximated as effectively constant for  $M \lesssim 10^9$  g. Thus, for  $M$  in this regime, we may take  $\varepsilon(M) \approx \varepsilon$ . It therefore follows from Eq. (2.7) that at time  $t$ , the mass  $M$  of a PBH produced at time  $t_i$  with initial mass  $M_i$  is given by

$$M = M_i \left[ 1 - \frac{t - t_i}{\tau(M_i)} \right]^{1/3} \Theta\left(\tau(M_i) - (t - t_i)\right), \quad (2.8)$$

where  $\Theta(x)$  denotes the Heaviside function of  $x$  and where

$$\tau(M_i) \equiv \frac{M_i^3}{3\varepsilon M_P^4} \quad (2.9)$$

is the lifetime  $\tau$  of the black hole — *i.e.*, the time after  $t_i$  at which  $M$  reaches zero.

### C. Evolution of the Energy Density

Once an initial spectrum  $f_{\text{BH}}(M_i, t_i)$  of PBHs is established at time  $t_i$ , this distribution evolves with time as a result of both evaporation and cosmic expansion. However, the comoving number density of PBHs with initial masses in the infinitesimal range from  $M_i$  to  $M_i + dM_i$  remains constant until  $t = \tau(M_i) + t_i$ , at which point the PBHs evaporate completely and the number density drops to zero. This implies that

$$a^3 f(M, t) dM = a_i^3 \Theta\left(\tau(M_i) - (t - t_i)\right) f(M_i, t_i) dM_i, \quad (2.10)$$

where  $a_i$  is the scale factor at time  $t_i$ .

The total energy density

$$\rho_{\text{BH}}(t) = \int_0^\infty dM f_{\text{BH}}(M, t) M \quad (2.11)$$

of the PBH population evolves with  $t$  according to the Boltzmann equation<sup>1</sup>

$$\frac{d\rho_{\text{BH}}}{dt} + 3H\rho_{\text{BH}} = \int_0^\infty dM f_{\text{BH}}(M, t) \frac{dM}{dt}, \quad (2.12)$$

<sup>1</sup> For a complete description of the PBH spectrum and its dynamical evolution which incorporates black-hole spins as well as masses, see Ref. [?] .

where  $dM/dt$  is given by Eq. (2.7). The conservation relation in Eq. (2.10) permits us to recast the integral over PBH masses  $M$  at time  $t$  on the right side of this equation as an integral over the corresponding initial masses  $M_i$ . In particular, we find that

$$\frac{d\rho_{\text{BH}}}{dt} + 3H\rho_{\text{BH}} = \left(\frac{a_i}{a}\right)^3 \int_{\widetilde{M}_i(t)}^\infty dM_i f_{\text{BH}}(M_i, t_i) \frac{dM}{dt}, \quad (2.13)$$

where  $dM/dt$  is understood to be an implicit function of  $M_i$  by virtue of the functional map between  $M$  and  $M_i$  in Eq. (2.8) and where

$$\widetilde{M}_i(t) \equiv \left[ 3\varepsilon M_P^4 (t - t_i) \right]^{1/3}. \quad (2.14)$$

This lower limit of integration arises from the Heaviside function in Eq. (2.10) and accounts for the fact that PBHs with masses  $M_i < \widetilde{M}_i(t)$  evaporate completely by time  $t$  and therefore no longer contribute to the energy density.

### D. Cosmological Dynamics and the Emergence of Stasis

We are now ready to examine the cosmological implications of a population of evaporating PBHs. In so doing, we shall follow as closely as possible the presentation in Ref. [39] concerning the general possibility of stasis between matter and radiation. The special case in which the matter comprises a population of PBHs and the radiation is produced through their evaporation was also previously discussed in Ref. [38].

For simplicity, we consider a flat Friedmann-Robertson-Walker (FRW) universe consisting of two cosmological components. The first is a population of PBHs characterized by a total energy density  $\rho_{\text{BH}}$  and corresponding total abundance

$$\Omega_{\text{BH}} \equiv \frac{8\pi G}{3H^2} \rho_{\text{BH}}. \quad (2.15)$$

The second is a radiation component characterized by an energy density  $\rho_\gamma$  and a corresponding abundance  $\Omega_\gamma = \Omega_{\text{BH}} - 1$ . The time-evolution of the PBH abundance is given by

$$\frac{d\Omega_{\text{BH}}}{dt} = \frac{8\pi G}{3} \left( \frac{1}{H^2} \frac{d\rho_{\text{BH}}}{dt} - 2 \frac{\rho_{\text{BH}}}{H^3} \frac{dH}{dt} \right), \quad (2.16)$$

where  $d\rho_{\text{BH}}/dt$  is given by Eq. (2.12) and where  $dH/dt$  is given by the Friedmann acceleration equation, which in this case takes the form

$$\frac{dH}{dt} = -H^2 - \frac{4\pi G}{3} \left[ \rho_{\text{BH}}(1 + 3w_{\text{BH}}) + \rho_\gamma(1 + w_\gamma) \right], \quad (2.17)$$

where  $w_{\text{BH}}$  and  $w_\gamma$  are the equation-of-state parameters for black holes and radiation, respectively. Since  $w_{\text{BH}} = 0$

and  $w_\gamma = 1/3$ , this equation reduces to [39]

$$\frac{dH}{dt} = -\frac{1}{2}H^2(4 - \Omega_{\text{BH}}). \quad (2.18)$$

Substituting this result for  $dH/dt$  into Eq. (2.16), we obtain

$$\frac{d\Omega_{\text{BH}}}{dt} = -\Gamma_{\text{BH}}(t)\Omega_{\text{BH}} + H(\Omega_{\text{BH}} - \Omega_{\text{BH}}^2), \quad (2.19)$$

where we have defined the effective BH evaporation rate

$$\begin{aligned} \Gamma_{\text{BH}}(t) &\equiv -\frac{\int_0^\infty f_{\text{BH}}(M, t) \frac{dM}{dt} dM}{\int_0^\infty f_{\text{BH}}(M, t) M dM} \\ &= -\frac{d}{dt} \log \left( \int_{\widetilde{M}_i(t)}^\infty f_{\text{BH}}(M_i, t_i) M(t) dM_i \right). \end{aligned} \quad (2.20)$$

For an initial PBH spectrum  $f_{\text{BH}}(M_i, t_i)$  of the form given in Eq. (2.2), this expression becomes

$$\Gamma_{\text{BH}}(t) \equiv -\frac{d}{dt} \log \left( \int_{\mu_i(t)}^{M_{\text{max}}} M_i^{\alpha-1} [M_i^3 - \widetilde{M}_i^3(t)]^{1/3} dM_i \right), \quad (2.21)$$

where  $\mu_i(t) \equiv \max\{M_{\text{min}}, \widetilde{M}_i(t)\}$ . While Eq. (2.21) is exact, we note that once  $\widetilde{M}_i(t) > M_{\text{min}}$  and the lightest PBHs begin to evaporate, this expression reduces to a particularly simple form in the regime in which  $\widetilde{M}_i(t) \ll M_{\text{max}}$ . In this regime, the value of the integral over  $M_i$  in Eq. (2.21) will not be significantly impacted by taking  $M_{\text{max}} \rightarrow \infty$ . Thus, in this regime  $\Gamma_{\text{BH}}(t)$  can be approximated as

$$\begin{aligned} \Gamma_{\text{BH}}(t) &\approx -\frac{d}{dt} \log \left( \int_{\widetilde{M}_i(t)}^\infty M_i^{\alpha-1} [M_i^3 - \widetilde{M}_i^3(t)]^{1/3} dM_i \right) \\ &\approx -\frac{\alpha+1}{3(t-t_i)}. \end{aligned} \quad (2.22)$$

Taken together, the differential equations in Eqs. (2.18) and (2.19) with  $\Gamma_{\text{BH}}(t)$  given in Eq. (2.21) describe the evolution of the PBH abundance. However, it is possible (and indeed particularly useful) to express this dynamics in terms of the dynamical variables  $\Omega_{\text{BH}}$  and its time-averaged value

$$\langle \Omega_{\text{BH}} \rangle \equiv \frac{1}{t-t_i} \int_{t_i}^t dt' \Omega_{\text{BH}}(t') \quad (2.23)$$

where the time averaging extends over the interval  $(t_i, t)$  where  $t_i$  is the initial time  $t_i$  at which the PBHs were produced and their mass spectrum implicitly established. In particular, integrating Eq. (2.18) yields a relation between these two variables of the form

$$\frac{1}{H} - \frac{1}{H_i} = \frac{1}{2}(t-t_i)(4 - \langle \Omega_{\text{BH}} \rangle), \quad (2.24)$$

where  $H_i$  is the initial value of  $H$  at  $t = t_i$ . At times  $t \gg t_i$ , when  $H \ll H_i$ , this relation reduces to

$$H \approx \frac{2}{4 - \langle \Omega_{\text{BH}} \rangle} \frac{1}{t}. \quad (2.25)$$

Recasting the coupled differential equations which govern the evolution of the PBH abundance in terms of  $\Omega_{\text{BH}}$  and  $\langle \Omega_{\text{BH}} \rangle$  is then simply a matter of substituting this result for  $H$  into Eqs. (2.19) and (2.29). We thus obtain

$$\begin{aligned} \frac{d\Omega_{\text{BH}}}{dt} &= \frac{1}{t} \Omega_{\text{BH}} \left[ \frac{\alpha+1}{3} + \frac{2(1-\Omega_{\text{BH}})}{4 - \langle \Omega_{\text{BH}} \rangle} \right] \\ \frac{d\langle \Omega_{\text{BH}} \rangle}{dt} &= \frac{1}{t} (\Omega_{\text{BH}} - \langle \Omega_{\text{BH}} \rangle). \end{aligned} \quad (2.26)$$

One advantage of expressing these coupled equations in this form is that it is more readily apparent that they are autonomous. Indeed, we observe that by performing a change of variables from  $t$  to  $\log t$ , we can remove all explicit time-dependence from the right sides of both equations in Eq. (2.26).

A more important observation that follows from the dynamical equations in Eq. (2.26) is that this dynamical system has a *fixed-point* solution in which

$$\Omega_{\text{BH}} = \langle \Omega_{\text{BH}} \rangle = \overline{\Omega}_{\text{BH}} \quad (2.27)$$

for all time, where

$$\overline{\Omega}_{\text{BH}} = \frac{4\alpha+10}{\alpha+7}. \quad (2.28)$$

Indeed, any configuration in which Eq. (2.27) is satisfied for all time is a solution to the dynamical equations in Eq. (2.26). Within such a system, the abundance  $\Omega_{\text{BH}}$  remains fixed even though the universe continues to expand! The abundance of radiation within this universe must therefore remain fixed as well. This solution, originally observed for black-hole dynamics in Ref. [38], is an example of a general phenomenon called *cosmic stasis* [39] in which the universe contains non-trivial mixtures of different energy components but in which the relative abundances of these components remains fixed despite cosmological expansion. Indeed, the solution in Eq. (2.27) is a particular example of cosmic stasis between matter and radiation when the matter is comprised of PBHs and the radiation is the product of their Hawking evaporation. Within Ref. [39], cosmic stasis was identified in the context of cosmologies involving towers of decaying particles, such as arise in many models of BSM physics. Indeed, it was shown in Ref. [39] that stasis will emerge regardless of the kinds of particles considered so long as their decay widths obey certain scaling relations. The above analysis demonstrates that this remains true even for cosmologies involving decaying towers of primordial black holes!

It is straightforward to determine the properties of the universe corresponding to the stasis solution. For constant  $\Omega_{\text{BH}} = \overline{\Omega}_{\text{BH}}$ , we may integrate Eq. (2.18) directly

in order to obtain the functional form of  $H$  during stasis. In particular, we find that the Hubble parameter is given by

$$H = \left( \frac{2}{4 - \bar{\Omega}_{\text{BH}}} \right) \frac{1}{t}. \quad (2.29)$$

Likewise, since  $\bar{\Omega}_{\text{BH}}$  is only sensibly defined within the range  $0 \leq \bar{\Omega}_{\text{BH}} \leq 1$ , it follows from Eq. (2.28) that a value of  $\alpha$  within the range  $-5/2 \leq \alpha \leq -1$  is required in order to obtain stasis. Combining this constraint with the one in Eq. (2.4), we find that

$$-2 \leq \alpha \leq -1, \quad (2.30)$$

which corresponds to the range  $0 \leq w_c \leq 1$ , where  $w_c$  is the equation-of-state parameter during the epoch within which the population of PBHs is initially established. Finally, the effective equation-of-state parameter  $\bar{w}$  during such a stasis can also be obtained directly by substituting this value of  $\bar{\Omega}_{\text{BH}}$  from Eq. (2.28) into Eq. (2.29), yielding

$$\bar{w} = -\frac{\alpha + 1}{\alpha + 7}. \quad (2.31)$$

Thus, if we demand that  $\alpha$  satisfy the criterion in Eq. (2.30), we find that our stasis solution requires  $0 \leq \bar{w} \leq 1/5$ .

Our final observation from the dynamical equations in Eq. (2.26) is that the fixed-point solution in Eq. (2.27) is actually a *global attractor* [38, 39]. As we have indicated, the stasis solution in Eq. (2.27) is valid for all time, and therefore assumes initial conditions for the dynamical equations in Eq. (2.26) that also happen to satisfy Eq. (2.27). Indeed, this is a fine-tuned initial condition. However, in most actual situations, our initial conditions are highly unlikely to be fine-tuned in this way. It is nevertheless straightforward to demonstrate that the dynamical system will generally flow toward the stasis solution even if it does not begin there.

In order to see this, we solve the system of equations in Eq. (2.26) numerically. Towards this end, we shall consider all possible combinations of initial conditions  $\Omega_{\text{BH}}(t_i)$  and  $\langle \Omega_{\text{BH}} \rangle(t_i)$  within the domains  $0 \leq \{\Omega_{\text{BH}}(t_*), \langle \Omega_{\text{BH}} \rangle(t_*)\} \leq 1$ . In order to ensure that PBH evaporation persists until arbitrarily late times, we take  $M_{\text{max}} \rightarrow \infty$ . We emphasize that the manner in which the system evolves in this limit for any particular choice of  $\alpha$  is effectively identical to the way in which it evolves for finite  $M_{\text{max}}$  at times  $t \lesssim \tau(M_{\text{max}})$ . Moreover, for simplicity, we also assume that  $M_{\text{min}}$  is such that the lightest PBHs have already begun evaporating by the time  $t = t_*$ .

The results of this analysis are shown in Fig. 1 for the case in which  $\alpha = -7/4$ . The blue curves represent the trajectories along which the system evolves in the  $(\Omega_{\text{BH}}, \langle \Omega_{\text{BH}} \rangle)$ -plane for  $\Omega_{\text{BH}}$  and  $\langle \Omega_{\text{BH}} \rangle$  anywhere within their domains  $0 \leq \{\Omega_{\text{BH}}, \langle \Omega_{\text{BH}} \rangle\} \leq 1$ . The red dot in the figure indicates the fixed-point solution in Eq. (2.27),

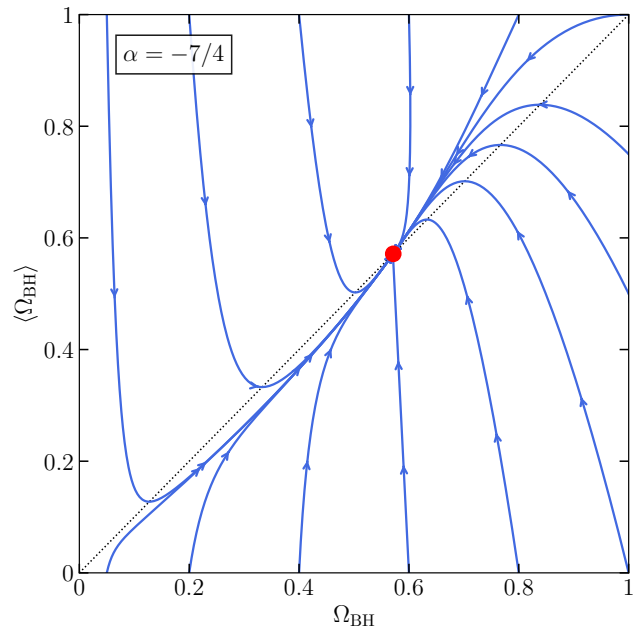


Fig. 1. Trajectories (blue curves) in the  $(\Omega_{\text{BH}}, \langle \Omega_{\text{BH}} \rangle)$ -plane for the system of differential equations in Eq. (2.26) with  $\alpha = -7/4$ . The red dot indicates the point at which  $\Omega_{\text{BH}} = \langle \Omega_{\text{BH}} \rangle = \bar{\Omega}_{\text{BH}}$ , where in this case  $\bar{\Omega}_{\text{BH}} \approx 0.57$ .

where in this case  $\bar{\Omega}_{\text{BH}} \approx 0.57$ . We observe that throughout the entirety of the plane, the system ultimately flows toward the stasis solution. Thus, we see that stasis is indeed a global attractor. Similar behavior arises for other choices of  $\alpha$  within the range given in Eq. (2.30).

At first glance, it might seem that this analysis is misleading because the dynamical equations in Eq. (2.26) are valid only at times  $t \gg t_i$ . It might therefore seem that we can only use these equations to study a possible *late-time* approach to stasis — *i.e.*, to study the dynamics starting at some fiducial time  $t_* \gg t_i$ . This in turn would imply that we are ignoring the possible non-trivial dynamics that occurred during the time interval from  $t_i$  to  $t_*$ . However, *regardless* of whatever non-trivial dynamics might have transpired between  $t_i$  and  $t_*$ , our system at  $t = t_*$  must nevertheless still lie somewhere within the  $(\Omega_{\text{BH}}, \langle \bar{\Omega}_{\text{BH}} \rangle)$  plane by the time our fiducial time  $t_*$  is reached, since this plane includes all possible values for these parameters. Our analysis then ensures that our system will subsequently be drawn to the stasis point.

We conclude, then, that the stasis solution is actually a global attractor within a cosmology of this type [38, 39]. Indeed, the primary message of Fig. 1 is not that it is merely *possible* for stasis to arise in cosmological scenarios involving PBHs, but that stasis is in fact a *generic feature* of cosmologies with certain physically motivated PBH mass spectra. Indeed, we have seen that stasis generically arises in *any* cosmological scenario in which a population of PBHs with a mass spectrum of the form

given in Eq. (2.2) with  $-2 \leq \alpha \leq -1$  is generated with a sizable initial abundance after inflation.

### III. STASIS IN THE EARLY UNIVERSE: STASIS IS NOT ETERNAL

Given the emergence of cosmological stasis arising from PBH decay, as discussed in Sect. IID, the primary goal of this paper is to understand the numerous phenomenological implications which follow. The first of our observations — indeed, the subject of this section — is that stasis itself does not last forever. Even though we have seen that stasis is an attractor, stasis ultimately persists for only a finite duration. As stressed in Ref. [39], this is a critical feature associated with stasis, allowing the universe to *exit* stasis as naturally as it enters it. *Indeed, without the ability to exit stasis in a natural way, the universe would have been trapped in an eternal stasis which would clearly be in conflict with direct observations of the present-day universe.* In this section we therefore discuss the entrance into *and exit from* stasis, with the goal of ultimately obtaining an expression for the number of  $e$ -folds across which a stasis epoch will last.

In order to set the stage for our analysis, we begin by considering the behavior of the PBH abundance  $\Omega_{\text{BH}}$  as a function of time. In Fig. 2 we plot  $\Omega_{\text{BH}}$  (solid curves) as functions of the number  $\mathcal{N}$  of  $e$ -folds for the PBH spectra corresponding to different choices of  $\alpha$ . In each case we have taken  $M_{\text{min}} = 10^{-1}$  g and  $M_{\text{max}} = 10^9$  g. We note that all of these choices lie within the range of physically meaningful values specified in Eq. (2.4) except for  $\alpha = -9/4$ , which we have included for purposes of illustration. In each case, we evaluate  $\Omega_{\text{BH}}(t)$  using the publicly-available code FRISBHEE [90]. For simplicity, we follow Ref. [39] in what follows by focusing on the case in which  $\Omega_{\text{BH}}(t_i) = 1$  — *i.e.*, the case in which the universe is initially dominated by PBHs. For concreteness, we also evaluate  $\varepsilon(M)$  by taking the particle content of the theory to be that of the Standard Model (SM). However, we note that the presence of a small number of additional light particle species in the theory would not have a significant effect on our results.

Regardless of the value of  $\alpha$ , we see that all of these curves share certain common characteristics. First, although they each begin at  $\Omega_{\text{BH}}(t_i) = 1$ , they each begin to fall below unity at a rate which initially increases with decreasing  $\alpha$ . In other words, the more negative  $\alpha$  becomes, the more steeply  $\Omega_{\text{BH}}(t)$  initially begins to fall.

Second, we see that in each case this falling behavior ultimately begins to level out, with each curve approaching a period of stasis. This is consistent with the idea that stasis is an attractor. Indeed, we see that the number of  $e$ -folds until stasis is reached also depends on  $\alpha$ , with more negative values of  $\alpha$  corresponding to more  $e$ -folds until stasis is achieved.

Third, we see that in each case our curve for  $\Omega_{\text{BH}}(t)$  then enters a period of stasis. During this period  $\Omega_{\text{BH}}(t)$

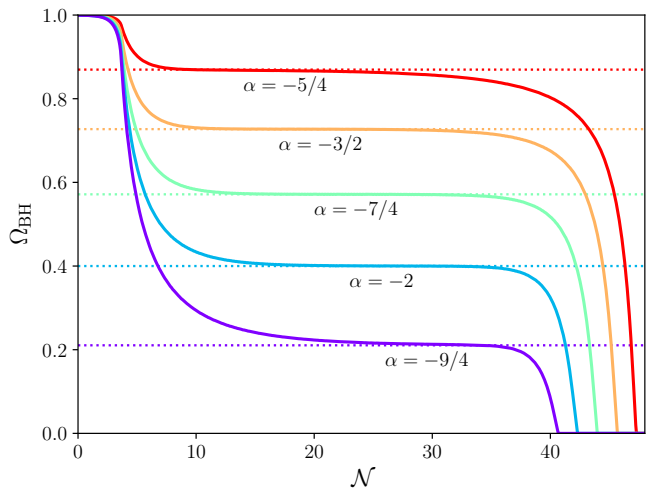


Fig. 2. The total abundance  $\Omega_{\text{BH}}$  of a population of PBHs with an initial mass spectrum of the form given in Eq. (2.2), plotted as a function of the number of  $e$ -folds  $\mathcal{N}$  of cosmic expansion since  $t_i$  for several different choices of the power-law exponent  $\alpha$  (solid curves). For all of the curves shown, we have taken  $M_{\text{min}} = 10^{-1}$  g and  $M_{\text{max}} = 10^9$  g. In each case, we see that the universe experiences a period of stasis stretching over many  $e$ -folds. Indeed, for each curve, the dotted line of the corresponding color represents the theoretical prediction in Eq. (2.28) for the PBH abundance  $\bar{\Omega}_{\text{BH}}$  during stasis.

— and therefore also  $\Omega_\gamma(t)$  — remain effectively constant, despite the effects of cosmic expansion. Indeed, in each case the stasis abundance  $\bar{\Omega}_{\text{BH}}$  precisely matches the prediction in Eq. (2.28). These latter predictions are indicated with dashed horizontal lines in Fig. 2.

But perhaps most importantly, we see that in each case this period of stasis is of only finite duration. Indeed, stasis ends in each case once the heaviest PBHs ultimately evaporate, whereupon the conversion of matter to radiation ceases. Given the curves in Fig. 2, we see that the number of  $e$ -folds across which stasis extends decreases with  $\alpha$ , such that more negative values of  $\alpha$  lead to shorter durations of stasis. We shall quantify this observation shortly.

Finally, once released from stasis, we find that in each case  $\Omega_{\text{BH}}(t)$  immediately begins to drop again, ultimately reaching  $\Omega_{\text{BH}} = 0$  once all of the PBHs have evaporated. Indeed, these curves do not asymptote to  $\Omega_{\text{BH}} = 0$ , as might have been expected, but instead hit zero with non-zero slope.

The basic dynamical considerations which give rise to the stasis behavior that we observe in Fig. 2 are the same as those which give rise to stasis in cosmologies involving decaying particles [39]. In a FRW universe, the energy density of radiation is diluted more quickly than that of matter as the universe expands; thus, the abundance of matter typically tends to increase over time, while the abundance of radiation tends to decrease. However, Hawking radiation counteracts this tendency by trans-

ferring energy from matter to radiation — a function analogous to the one the particle decays play within the realization of stasis presented in Ref. [39]. The interplay between these two effects drives the universe toward a steady state in which the abundances of matter and radiation remain effectively constant in time. Indeed, the stasis epoch which arises from a population of evaporating PBHs is of finite duration only because there exists a cutoff  $M_{\max}$  in the initial PBH mass spectrum — a cutoff which in turn implies a maximum lifetime  $\tau(M_{\max})$  for any PBH within that population.

That said, we stress that the dynamics of PBH evaporation discussed in Sect. II is fundamentally different from the dynamics of particle decay in a number of ways. For one thing, the form of the collision term in the Boltzmann equation which describes the transfer of energy density from matter to radiation for a population of decaying particles of the same species  $\phi$  differs from the form of the corresponding collision term for a population of PBHs with a common initial mass  $M_i$ . In the decaying-particle case, this collision term takes the form  $\mathcal{C}_\phi = -\Gamma_\phi \rho_\phi$ , where  $\rho_\phi$  is the energy density of the particles and where  $\Gamma_\phi$  is their proper decay width. By contrast, in the PBH case, the collision term is the product of the number density  $n_{\text{BH}}$  associated with this monochromatic spectrum of PBHs and the evaporation rate in Eq. (2.7). Expressed in terms of the corresponding energy density  $\rho_{\text{BH}} \approx M n_{\text{BH}}$ , the collision term in this case takes the form

$$\mathcal{C}_{\text{BH}} = -\varepsilon(M) \frac{M_P^4}{M^3} \rho_{\text{BH}}. \quad (3.1)$$

The factor  $\varepsilon(M)M_P^4/M^3$  multiplying the energy density in this expression grows with time as the mass of each individual PBH decreases according to Eq. (2.14) until  $t - t_i = \tau(M_i)$ , at which point the PBHs evaporate completely. Since the corresponding factor  $\Gamma_\phi$  in the decaying-particle case is constant, it follows that the energy density of PBHs falls more precipitously when  $t - t_i \sim \tau(M_i)$  than does the energy density of decaying particles when  $t - t_i \sim 1/\Gamma_\phi$ .

Another significant difference between particle decay and PBH evaporation involves the sequence in which different states transfer their energy to radiation. In general, heavier particles with the same quantum numbers tend to decay before lighter ones. This causes the conversion from matter to radiation to proceed *down* the tower of states in the sense that progressively lighter states dominate the rate at which rest energy is transferred to radiation as time evolves. By contrast, for PBHs the reverse is true: lighter PBHs lose their energy to radiation more rapidly than heavier ones. As a result, the conversion from matter to radiation proceeds *up* the PBH tower in the sense that states with progressively larger initial masses  $M_i$  dominate the rate at which rest energy is transferred to radiation as time evolves.

Finally, we may derive an approximate expression for the *duration* of the stasis epoch. The transfer of energy

density from matter to radiation on which stasis relies only occurs at a significant rate once the lightest PBHs in the tower begin to evaporate completely. Thus, the window during which PBH evaporation gives rise to stasis is roughly  $\tau(M_{\min}) \lesssim t \lesssim \tau(M_{\max})$ . The corresponding number of  $e$ -folds is

$$\mathcal{N}_s \approx \log \left[ \frac{a(\tau(M_{\max}))}{a(\tau(M_{\min}))} \right]. \quad (3.2)$$

During stasis, the scale factor scales with time according to the relation  $a(t) \propto t^{2/(3\bar{w}+3)}$ , with  $\bar{w}$  given by Eq. (2.31). Thus, we find that the number of  $e$ -folds of stasis to which a population of evaporating PBHs gives rise is

$$\mathcal{N}_s \approx \frac{\alpha + 7}{3} \log \left( \frac{M_{\max}}{M_{\min}} \right). \quad (3.3)$$

We note that Eq. (3.3) can be used in order to derive a rough upper bound on the number of  $e$ -folds of cosmic stasis which can be achieved through PBH evaporation in scenarios in which the PBHs are produced by the collapse of primordial density fluctuations after inflation. As discussed in Sect. II, both  $M_{\min}$  and  $M_{\max}$  are constrained in such scenarios to lie within the range specified in Eq. (2.5). Taking  $M_{\min}$  at the lower limit of this range and  $M_{\max}$  at the upper limit yields a rough upper bound on  $\mathcal{N}_s$  of the form

$$\mathcal{N}_s \lesssim 23 \left( \frac{\alpha + 7}{3} \right). \quad (3.4)$$

Thus, even under the conservative assumptions which led to Eq. (2.5), we observe that a significant number of  $e$ -folds of stasis — up to  $\mathcal{N}_s \approx 38.3$  for  $\alpha = -2$ , and even more for larger values of  $\alpha$  — can be achieved through PBH evaporation. Thus, in cosmologies involving evaporating PBHs, stasis can extend over a potentially significant portion of the cosmological timeline.

As indicated above, the fact that a period of stasis has at most a finite duration implies that our universe is not only inevitably drawn into a period of stasis but also naturally expelled from it. Thus it makes sense to speak of a stasis “epoch”, one which might resemble a matter- or radiation-dominated epoch in having a constant equation of state except that this epoch comprises non-trivial amounts of matter and radiation simultaneously and therefore has a non-traditional equation of state. This is therefore a new kind of cosmological epoch — one which is an intrinsic feature of universes that give rise to an appropriate spectrum of PHBs at early times. It is therefore important to understand the phenomenological implications of such a stasis epoch.

#### IV. PHENOMENOLOGICAL IMPLICATIONS OF PBH-INDUCED STASIS

In this section we shall consider some of the phenomenological implications of a stasis epoch induced by



PBH evaporation. These will include the effects of such an epoch on the cosmic expansion history, on inflation, on gravitational waves, on dark radiation, on dark matter, and on baryogenesis. Needless to say, many of these effects are interconnected. We shall nevertheless attempt to separate the relevant physics into distinct discussions as much as possible.

### A. Cosmic Expansion History

In the previous sections, we have shown that the evaporation of a population of PBHs with a mass spectrum described by the power-law distribution in Eq. (2.2) can give rise to a stasis epoch lasting a significant number of  $e$ -folds. Such a modification of the cosmic expansion history can have an impact on variety of astrophysical quantities, including the spectrum of primordial density fluctuations and the stochastic gravitational-wave (GW) background.

In this section, we examine the phenomenological implications of modified cosmologies involving a stasis epoch induced by PBH evaporation. We begin by reviewing the expansion history of the universe that characterizes cosmologies of this sort from the end of inflation to the present time. This expansion history includes not only a stasis epoch, but the entire sequence of epochs described below.

- Immediately following inflation, the universe is dominated by a perfect fluid with an equation-of-state parameter  $0 \leq w_c \leq 1$ . PBHs form after inflation via the gravitational collapse of primordial density perturbations during this epoch. The power spectrum of these perturbations is assumed to be scale-invariant across the entire range of comoving wavenumbers  $k$  which correspond to PBH masses within the range  $M_{\min} \leq M_i \leq M_{\max}$ . As discussed in Sect. II, such a perturbation spectrum gives rise to an initial PBH mass spectrum of the form given in Eq. (2.2). We emphasize, however, that while we assume the power spectrum of these perturbations to be scale-invariant *within* this range of  $k$ , the amplitude of these perturbations may potentially be significantly enhanced relative to the amplitude of perturbations *outside* this range.
- Prior to the time at which these PBHs begin evaporating at a non-negligible rate, their abundance increases for  $w_c$  within this range. This eventually leads to a matter-dominated epoch during which the PBHs themselves dominate the energy density of the universe. The duration of this epoch — which we parametrize in terms of the number of  $e$ -folds of cosmic expansion  $\mathcal{N}_{\text{PBH}}$  that take place therein — depends on the total abundance of PBHs generated over the course of the preceding epoch. This abundance in turn depends fundamentally on

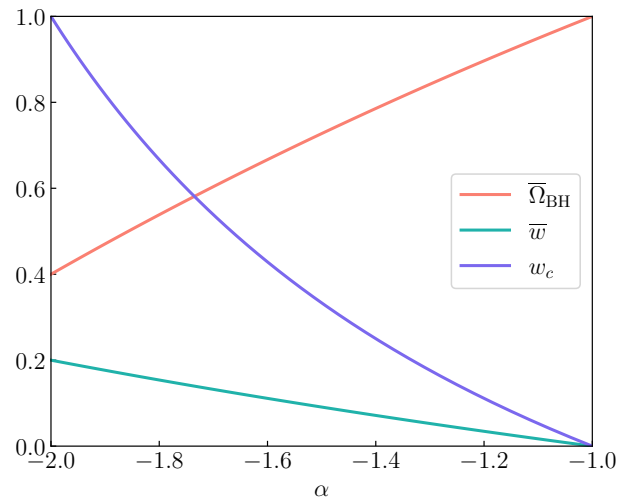


Fig. 3. The PBH abundance  $\bar{\Omega}_{\text{BH}}$  during stasis, the equation-of-state parameter  $\bar{w}$  during stasis, and the equation-of-state parameter  $w_c$  during the PBH-formation epoch, each plotted as a function of  $\alpha$ .

the amplitude of the primordial density perturbations which collapse to form the PBHs — an amplitude which, as discussed above, can potentially be significantly enhanced within the region of  $k$  relevant for PBH formation. We therefore take  $\mathcal{N}_{\text{PBH}}$  to be a free parameter in what follows.

- Once the PBHs begin evaporation, the universe evolves toward a stasis due to the attractor behavior discussed in Sect. IID. The effective equation-of-state parameter  $\bar{w}$  for the universe during the stasis epoch is given by Eq. (2.31) and the duration of this epoch is given by Eq. (3.3).
- After the heaviest PBHs have evaporated, the universe becomes radiation-dominated. The subsequent expansion history of the universe coincides with that of the standard cosmology.

We emphasize that the parameters  $w_c$ ,  $\bar{w}$ , and  $\alpha$  are not independent in cosmologies of this sort; rather, they are interrelated through Eqs. (2.3) and (2.31). The relationships between these three parameters are displayed graphically in Fig. 3. Thus, since the duration of the stasis epoch depends not only on  $\alpha$ , but also on the ratio  $M_{\max}/M_{\min}$ , the expansion history after inflation in these kinds of modified cosmologies is determined by two parameters, which we take to be  $\alpha$  and  $M_{\max}/M_{\min}$ .

Since the equation-of-state parameter is constant during each of the individual cosmological epochs described above, it is straightforward to obtain the total number of  $e$ -folds of expansion which take place between the end of inflation and present time. In particular, in the approximation that transitions between successive cosmological epochs may be considered effectively instantaneous, the

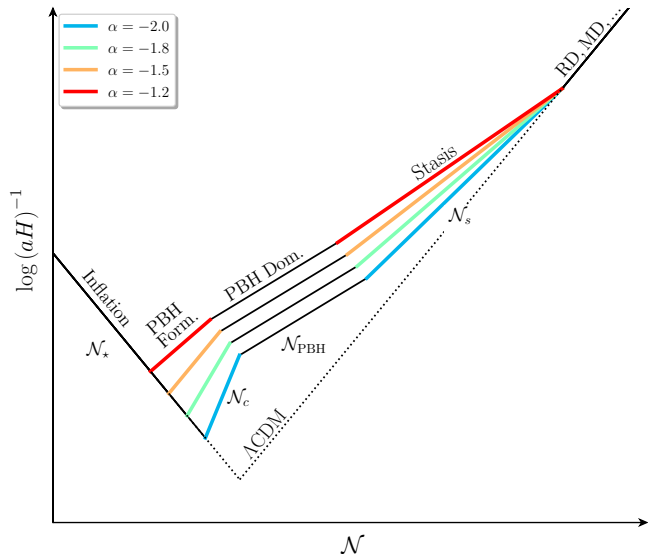


Fig. 4. Qualitative sketch illustrating how the comoving Hubble horizon evolves in cosmologies involving an epoch of PBH-induced stasis as a function of the number of  $e$ -folds for several different values of  $\alpha$ . All curves shown correspond to the parameter choices  $M_{\max}/M_{\min} = 10^{10}$  and  $\mathcal{N}_{\text{PBH}} = 15$ . The evolution of  $(aH)^{-1}$  in the standard cosmology is indicated by the dotted black curve.

number of  $e$ -folds of expansion which take place during an epoch with equation-of-state parameter  $w_j$  is related to the values  $H_j$  and  $H_{j+1}$  of the Hubble parameter at the beginning of that epoch and at the beginning of the subsequent epoch, respectively, by

$$\mathcal{N}_j = \frac{2}{3(1+w_j)} \log\left(\frac{H_{j+1}}{H_j}\right). \quad (4.1)$$

Given a particular set of input parameters  $\alpha$ ,  $M_{\min}$ ,  $M_{\max}$ , and  $\mathcal{N}_{\text{PBH}}$  and a value of  $H_{\text{end}}$  at the end of inflation, this relation is sufficient to allow us to reconstruct the entire expansion history.

The manner in which the comoving Hubble horizon evolves in modified cosmologies of this sort from the end of inflation until the present time is shown in Fig. 4 for a variety of different values of  $\alpha$  within the physically motivated range given in Eq. (2.4). For each of the curves shown, we have taken  $M_{\max}/M_{\min} = 10^{10}$ , which yields the maximal duration for the stasis epoch consistent with Eq. (2.5) for a given value of  $\alpha$ . We have also taken  $\mathcal{N}_{\text{PBH}} = 15$ . The manner in which  $(aH)^{-1}$  evolves in the standard cosmology is indicated by the dotted black line.

The results shown in Fig. 4 illustrate that in cosmologies involving an epoch of PBH-induced stasis,  $(aH)^{-1}$  can depart significantly from the corresponding result in the standard cosmology between the end of inflation and the end of the stasis epoch, and that this departure becomes more pronounced as  $\alpha$  increases. Indeed, this modified evolution of the comoving Hubble radius is ultimately responsible for many of the phenomenological

signatures of PBH-induced stasis which we shall discuss below.

## B. Inflation

Cosmic inflation stands as one of the most compelling frameworks that can explain the extraordinary homogeneity of the cosmic microwave background (CMB) while generating from quantum fluctuations the metric perturbations that led to structure formation later in cosmic history [87, 91–93]. In its simplest realizations, a scalar field slowly rolling along its potential is responsible for generating the perturbation modes which give rise to the pattern of inhomogeneities observed in the CMB. In order to derive a theoretical prediction for this pattern of inhomogeneities in the context of a given inflationary model, one must determine the values of the so-called slow-roll parameters at the time at which the relevant perturbation modes exited the Hubble horizon. However, the value of the scale factor at this time is entirely dependent on the subsequent expansion history of the universe. As discussed in Ref. [39], the presence of a cosmic stasis epoch within the cosmological timeline can affect the number of  $e$ -folds of cosmic expansion which occur between the time at which these modes exit the horizon and the time at which they reenter. In this subsection, we examine the impact that the presence of a PBH-induced stasis epoch — along with the other modifications of the expansion history involved in establishing such an epoch — has on predictions for inflationary observables which can be inferred from the properties of the CMB.

The primary inflationary observables of this sort are the spectral index  $n_s$  and the tensor-to-scalar ratio  $r$  which characterize the spectrum of primordial perturbations, evaluated at some chosen pivot scale  $k_*$ . In order to make contact with observation, we adopt the pivot scale  $k_* = 0.002 \text{ Mpc}^{-1}$  used in the analysis performed by the Planck Collaboration [94]. In slow-roll inflation scenarios, these observables are related to the scalar potential  $V(\phi)$  for the inflaton field  $\phi$  through the slow-roll parameters

$$\begin{aligned} \epsilon &\equiv \frac{M_{\text{P}}^2}{16\pi} \left[ \frac{V'(\phi_*)}{V(\phi_*)} \right]^2 \\ \eta &\equiv \frac{M_{\text{P}}^2}{8\pi} \left| \frac{V''(\phi_*)}{V(\phi_*)} \right|, \end{aligned} \quad (4.2)$$

where a prime denotes a derivative with respect to  $\phi$  and where  $\phi_*$  denotes the value of  $\phi$  at the time at which the mode with wavenumber  $k_*$  exits the horizon. In particular, in such scenarios, one finds that

$$\begin{aligned} n_s &= 1 - 6\epsilon + 2\eta \\ r &= 16\epsilon. \end{aligned} \quad (4.3)$$

The value of  $\phi_*$  depends sensitively on the expansion history of the universe after inflation. For a given expan-

sion history, the value of  $\phi_*$  may be determined as follows [50, 95–99]. The number of  $e$ -folds of expansion  $\mathcal{N}_*$  that the universe undergoes between the time at which the perturbation mode with comoving wavenumber  $k_*$  exits the horizon and the end of inflation using the relation

$$k_* = a_* H_* = e^{-\mathcal{N}_*} a_{\text{end}} H_*, \quad (4.4)$$

where  $a_*$  and  $H_*$  respectively denote the values of the scale factor and the Hubble parameter at the moment at which this mode exits the horizon, and where  $a_{\text{end}}$  denotes the value of the scale factor at the end of inflation. In the slow-roll approximation,  $H_*$  and  $\phi_*$  are related by

$$H_*^2 \approx \frac{8\pi V(\phi_*)}{3M_P^2}. \quad (4.5)$$

On the other hand, the slow-roll approximation also implies that

$$\mathcal{N}_* \approx \log\left(\frac{a_{\text{end}}}{a_*}\right) = \frac{8\pi}{M_P^2} \int_{\phi_{\text{end}}}^{\phi_*} \frac{V(\phi)}{V'(\phi)} d\phi. \quad (4.6)$$

Taken together, Eqs. (4.4), (4.5), and (4.6) yield an integro-differential equation of the form

$$\frac{8\pi}{M_P^2} \int_{\phi_{\text{end}}}^{\phi_*} \frac{V(\phi)}{V'(\phi)} d\phi = \frac{1}{2} \log\left(\frac{8\pi a_{\text{now}}^2 V(\phi_*)}{3M_P^2 k_*^2}\right) - \log\left(\frac{a_{\text{now}}}{a_{\text{end}}}\right), \quad (4.7)$$

which can be solved numerically for  $\phi_*$ . It is through the second term on the right side of Eq. (4.7) — which represents the total number of  $e$ -folds of expansion that occur between the end of inflation and the present time — that  $\phi_*$  depends on the expansion history after inflation.

The results for  $n_s$  and  $r$  of course depend on the form of the inflaton potential as well as on the expansion history of the universe after inflation. Here, for concreteness, we focus on two commonly studied classes of inflaton potentials. The first are polynomial potentials which take the form

$$V(\phi) \sim |\phi|^p \quad (4.8)$$

for some value of  $p$ . The second consists of so-called  $T$ -model  $\alpha$ -attractors [100], for which the inflaton potential takes the form

$$V(\phi) \sim \tanh^{2n} \left( \sqrt{\frac{4\pi}{3\alpha_{\text{inf}}}} \frac{\phi}{M_P} \right), \quad (4.9)$$

where  $n$  and  $\alpha_{\text{inf}}$  are dimensionless free parameters. We focus here on the case in which  $n = 1$ , for which this form of  $V(\phi)$  coincides with the inflaton potential characteristic of Starobinsky  $R^2$  models [101, 102].

In Fig. 5 we display the results obtained for  $n_s$  and  $r$  in a cosmology involving an epoch of PBH-induced stasis as points in the  $(n_s, r)$ -plane for the two classes of inflaton

potential given in Eqs. (4.8) and (4.9). Each sequence of points appearing on the left side of the figure corresponds to a potential of the form given in Eq. (4.9) with a different value  $\alpha_{\text{inf}}$ . Likewise, each sequence of points appearing on the right side of the figure corresponds to a different value of the parameter  $p$  in Eq. (4.8). The color of each point within a particular such sequence indicates the value of the parameter  $\alpha$  in Eq. (2.2). In all cases, we have taken  $M_{\text{min}} = 0.1 \text{ g}$  and  $M_{\text{max}} = 10^9 \text{ g}$ , such that the value of  $\mathcal{N}_s$  is maximized for each choice of  $\alpha$ . We have also taken  $\mathcal{N}_{\text{PBH}} = 5$ . Taken together, these choices of  $M_{\text{min}}$ ,  $M_{\text{max}}$ , and  $\mathcal{N}_{\text{PBH}}$  specify the duration of the PBH-formation epoch. The regions within which the values of  $n_s$  and  $r$  are consistent with Planck data [94] at the 68% and 95% CL are shaded dark and light blue, respectively. The dark- and light-purple regions represent the corresponding 68% and 95% CL projections for CMB-S3 experiments such as the Simons Observatory [103] and the South Pole Observatory [104] collectively, while the dark- and light-red regions represent the corresponding projections for the CMB-S4 experiment [105].

We observe from Fig. 5 that the modifications of the expansion history associated with cosmologies involving a PBH-induced stasis epoch have a significant impact on the predictions for  $r$  and  $n_s$  obtained for a given inflaton potential. In general, these modifications have the effect of decreasing  $n_s$  and increasing  $r$  relative to the corresponding values obtained in the context the standard cosmology, and the larger the value of  $\alpha$  becomes, the more pronounced this effect becomes. For the  $T$ -model potential in Eq. (4.9), these modifications increase the tension between theoretical predictions for  $n_s$  and  $r$  and CMB data. Indeed, for  $\alpha \gtrsim -1.3$ , we find that the resulting prediction for  $n_s$  and  $r$  lie outside the Planck 95%-CL region for essentially all values of  $\alpha_{\text{inf}}$  we consider here. By contrast, for the polynomial potential in Eq. (4.8), the shift in  $n_s$  and  $r$  which results from the modification of the expansion history serves to partially ameliorate the tension between the predictions for these quantities and CMB data. Indeed, for large values of  $p$  the resulting shift in these quantities is sufficient to land them — though just barely — within the Planck 95%-CL region, thereby rendering a model which was disfavored by CMB (marginally) consistent with those measurements. We emphasize that the trends illustrated in Fig. 5 concerning the manner in which the values of  $n_s$  and  $r$  shift in cosmologies involving an epoch of PBH-induced stasis relative to their values in the standard cosmology are general and should apply in other inflationary models as well.

### C. Gravitational Waves

Both the presence of a PBH-induced stasis epoch within the cosmological timeline and the additional modifications of the expansion history involved in establishing such a stasis epoch also have a non-trivial impact

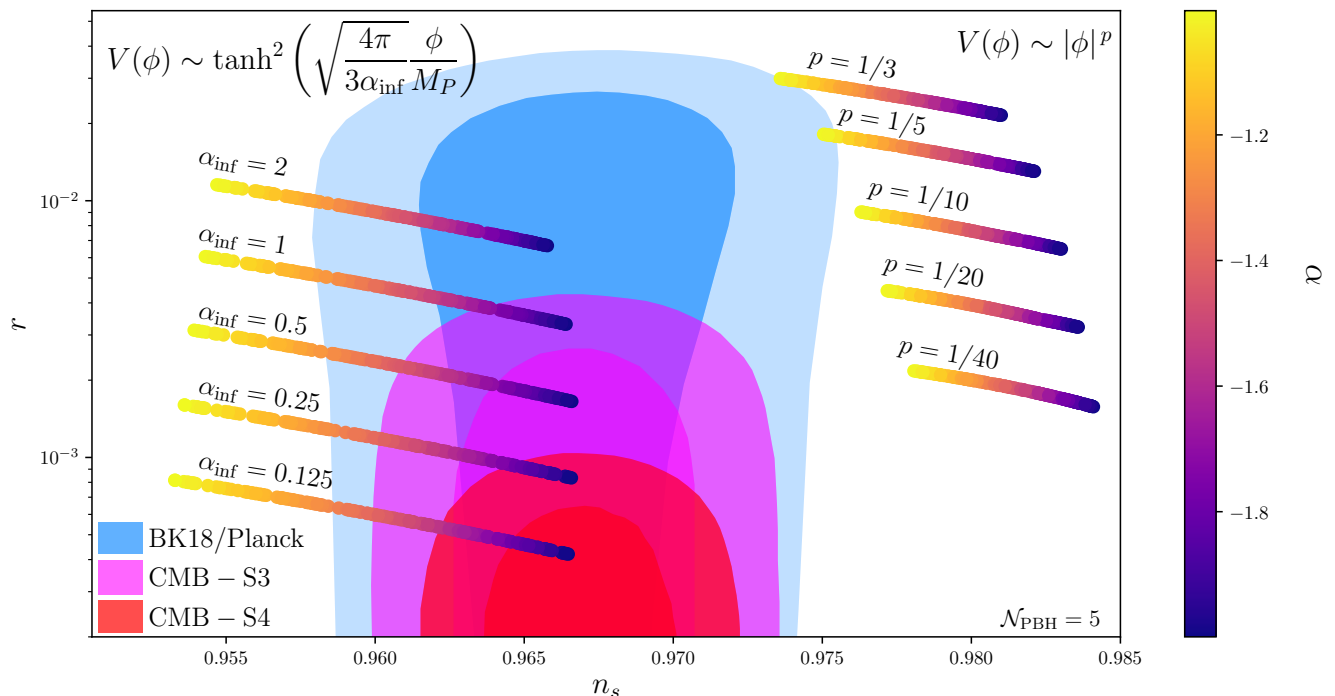


Fig. 5. The spectral index  $n_s$  and tensor-to-scalar ratio  $r$  in cosmologies involving an epoch of PBH-induced stasis, shown as points in the  $(n_s, r)$ -plane for the two classes of inflaton potential given in Eqs. (4.8) and (4.9). Each sequence of points appearing on the left side of the figure corresponds to a potential of the form given in Eq. (4.9) with a different value  $\alpha_{\text{inf}}$ . Each sequence of points appearing on the right side of the figure corresponds to a different value of the parameter  $p$  in Eq. (4.8). The color of each point within a particular such sequence indicates the value of the parameter  $\alpha$  in Eq. (2.2). For all points shown in the figure, we have taken  $M_{\text{min}} = 0.1$  g and  $M_{\text{max}} = 10^9$  g, such that the value of  $\mathcal{N}_s$  is maximized for each choice of  $\alpha$ . We have also taken  $\mathcal{N}_{\text{PBH}} = 5$ . The regions within which the values of  $n_s$  and  $r$  are consistent with Planck data [94] at the 68% and 95% CL are shaded dark and light blue, respectively. The dark- and light-purple regions represent the corresponding 68% and 95% CL projections for CMB-S3 experiments collectively, while the dark- and light-red regions represent the corresponding projections for CMB-S4 [105].

on the resulting present-day spectrum of GWs. Indeed, in cosmologies with modified expansion histories, this spectrum — defined more precisely as the differential present-day abundance  $d\Omega_{\text{GW}}/d\log f$  of GWs per unit logarithmic present-day frequency  $\log f$  — is modified relative to the present-day GW spectrum that would be obtained within the context of the standard cosmology for the same primordial spectrum of tensor perturbations [98, 106]. In particular, the manner in which  $d\Omega_{\text{GW}}/d\log f$  scales with  $f$  is modified across any range of  $f$  for which the GWs reenter the horizon during an epoch during which the universe is not radiation-dominated. In the cosmologies we consider here, such epochs include the stasis epoch itself, the epoch of PBH-domination which precedes it, and the epoch during which the PBHs are initially produced.

We begin by examining the impact of the cosmological modifications involved in our PBH-induced stasis scenario on contributions to the GW spectrum generated by other sources. For concreteness, we consider the case in which a stochastic background of GWs is established prior to the PBH-formation epoch. Under stan-

dard assumptions that this stochastic GW background (SGWB) is homogeneous, isotropic, Gaussian, and unpolarized, the differential energy density  $d\rho_{\text{GW}}(a)/d\log k$  of GWs per unit logarithmic comoving-wavenumber  $\log k$ , expressed as a function of the scale factor  $a$ , takes the form [107]

$$\frac{d\rho_{\text{GW}}(a)}{d\log k} = \frac{k^2 h_k^2(a)}{16\pi G a^2}, \quad (4.10)$$

where  $h_k(a)$  represents the characteristic differential amplitude of tensor perturbations to the spacetime metric per unit  $\log k$ , likewise expressed as a function of  $a$ . This differential amplitude evolves with  $a$  according to the relation

$$h_k(a) = \frac{a_k}{a} h_k(a_k), \quad (4.11)$$

where  $a_k$  denotes the value of  $a$  at the time at which a perturbation with comoving wavenumber  $k$  reenters the horizon.

In a flat universe, the Hubble parameter scales with  $a$  according to the proportionality relation  $H = \sqrt{8\pi G \rho} \propto$

$a^{-3(1+w)/2}$  during a cosmological epoch wherein the equation-of-state parameter  $w$  is effectively constant. The comoving wavenumber of the GW which enters the horizon during such an epoch therefore scales with  $a_k$  according to the proportionality relation

$$k = a_k H_k \propto a_k^{-(1+3w)/2}. \quad (4.12)$$

It therefore follows from Eqs. (4.10) and (4.11) that

$$\frac{d\rho_{\text{GW}}(a)}{d\log k} \propto a^{-4} h_k^2(a_k) k^{\xi(w)}, \quad (4.13)$$

where we have defined

$$\xi(w) \equiv \frac{2(3w-1)}{(3w+1)}. \quad (4.14)$$

Within the context of the standard cosmology (wherein the universe is radiation-dominated, with  $w = 1/3$ , from the end of reheating until the time of matter-radiation equality), Eq. (4.13) implies that  $d\rho_{\text{GW}}(a)/d\log k \propto h_k^2(a_k)$ . By contrast, within the context of any modified cosmology wherein the universe is *not* radiation-dominated throughout this interval, the resulting GW spectrum is distorted relative to this result. Indeed, we see that  $d\rho_{\text{GW}}(a)/d\log k$  increases more rapidly with  $k$  during an epoch wherein  $w > 1/3$  than it does in the standard cosmology, whereas it increases less rapidly than it does in the standard cosmology during an epoch wherein  $w < 1/3$ .

For concreteness, in order to illustrate how the modified expansion history associated with a PBH-induced stasis epoch affects the GW spectrum, we consider a spectrum of tensor perturbations for which the initial amplitude  $h_k(a_k)$  is independent of  $k$ . Such a spectrum of tensor perturbations arises generically in single-field inflation scenarios in which the spectrum of primordial curvature perturbations generated by inflation is perfectly scale invariant — *i.e.*, scenarios in which  $n_s = 1$ . For simplicity, we ignore any additional contributions to

the perturbation spectrum which might arise from other sources. We shall return to discuss the effect of such contributions later in this subsection.

For such an initial spectrum of tensor perturbations, the  $k$ -dependence of  $d\rho_{\text{GW}}/d\log k$  is determined solely by the expansion history. Over ranges of  $k$  for which GW modes reenter the horizon during radiation domination,  $d\rho_{\text{GW}}(a)/d\log k$  is “flat” — *i.e.*, independent of  $k$ . By contrast, over ranges of  $k$  for which GW modes reenter the horizon during any epoch wherein  $w \neq 1/3$ , this differential energy density varies with  $k$ , as discussed above. In the PBH-induced stasis scenario we are considering here, the epochs wherein  $w \neq 1/3$  include not only the epoch of PBH-induced stasis itself, but also the epoch during which the PBHs are initially produced and the subsequent epoch of PBH domination which immediately precedes stasis.

We now turn to assessing the potential consequences of these cosmological modifications for GW detection. The present-day GW spectrum is defined according to the relation

$$\frac{d\Omega_{\text{GW}}}{d\log f} \equiv \frac{1}{\rho_{\text{crit}}(a_{\text{now}})} \frac{d\rho_{\text{GW}}(a_{\text{now}})}{d\log f}, \quad (4.15)$$

where  $\rho_{\text{crit}}(a_{\text{now}})$  is the present-day value of the critical density of the universe and where  $d\rho_{\text{GW}}(a_{\text{now}})/d\log f$  is the differential present-day energy density of GWs per unit  $\log f$ . Since  $f = k/(2\pi a_{\text{now}})$ , where  $a_{\text{now}}$  denotes the present-day value of the scale factor, it follows that

$$\frac{d\rho_{\text{GW}}(a_{\text{now}})}{d\log f} = \frac{d\rho_{\text{GW}}(a_{\text{now}})}{d\log k}. \quad (4.16)$$

In the approximation that the transitions between different cosmological epochs may be taken to be effectively instantaneous, we find that  $d\Omega_{\text{GW}}/d\log f$  in a cosmology with an epoch of PBH-induced stasis is given by the piecewise function

$$\frac{d\Omega_{\text{GW}}}{d\log f} = \frac{d\Omega_{\text{GW}}^{\text{sc}}}{d\log f} \times \begin{cases} 1 & f \leq f_s \\ \left(\frac{f}{f_s}\right)^{\xi(\bar{w})} & f_s < f \leq f_{\text{PBH}} \\ \left(\frac{f_{\text{PBH}}}{f_s}\right)^{\xi(\bar{w})} \left(\frac{f}{f_{\text{PBH}}}\right)^{-2} & f_{\text{PBH}} < f \leq f_f \\ \left(\frac{f_{\text{PBH}}}{f_s}\right)^{\xi(\bar{w})} \left(\frac{f}{f_{\text{PBH}}}\right)^{-2} \left(\frac{f}{f_f}\right)^{\xi(w_c)} & f_f < f \leq f_{\text{end}} \\ 0 & f_{\text{end}} < f, \end{cases} \quad (4.17)$$

where  $d\Omega_{\text{GW}}^{\text{sc}}/d\log f$  denotes the GW spectrum obtained for the same spectrum of primordial tensor perturbations within the context of the standard cosmology and where  $f_{\text{end}}$ ,  $f_f$ ,  $f_{\text{PBH}}$ , and  $f_s$  respectively indicate the values of  $f$  associated with the GW modes which reenter the hori-

zon at the end of inflation; at the end of the epoch immediately following inflation during which the PBHs are initially produced; at the end of the ensuing epoch of PBH domination; and at the end of the stasis epoch. Since  $d\rho_{\text{GW}}(a)/d\log f$  is independent of  $f$  in the standard cos-

mology, the quantity  $d\Omega_{\text{GW}}^{\text{sc}}/d\log f$  may be viewed simply as an overall normalization factor in  $d\Omega_{\text{GW}}/d\log f$  — a normalization factor which takes the form [107]

$$\frac{d\Omega_{\text{GW}}^{\text{sc}}}{d\log f} = \Omega_\gamma(a_{\text{now}}) \left( \frac{g_{\star S}(T_{\text{eq}})}{g_{\star S}(T_k)} \right)^{4/3} \frac{g_\star(T_k)}{24\pi^2} \frac{H_\star^2}{M_P^2}, \quad (4.18)$$

where  $\Omega_\gamma(a_{\text{now}}) \simeq 5.38 \times 10^{-5}$  is the present-day photon abundance [108].

In Fig. 6, we show a variety of present-day GW spectra which arise in cosmologies involving a PBH-induced stasis epoch characterized by different combinations of the parameters  $\alpha$ ,  $M_{\text{min}}$ , and  $M_{\text{max}}$ . In the left panel, we display the GW spectra obtained for several different choices of  $\alpha$  within the physically allowed range in Eq. (2.30) for fixed  $M_{\text{min}} = 100$  g and  $M_{\text{max}} = 10^5$  g. By contrast, in the right panel, we display the GW spectra obtained for several different combinations of  $M_{\text{min}}$  and  $M_{\text{max}}$  for fixed  $\alpha = -2$  (a value of  $\alpha$  which corresponds to  $\bar{w} = 1/5$  and  $w_c = 1$ ). For each of the curves shown, we have taken  $H_\star = 2.5 \times 10^{-5} M_P$ , which saturates the upper bound on  $H_\star$  from CMB data [87]. For concreteness, we also take the number of  $e$ -folds during PBH domination to be  $\mathcal{N}_{\text{PBH}} = 2$ . The colored curves appearing in each panel indicate the GW spectra obtained for different choices of the parameters  $\alpha$ ,  $M_{\text{max}}$ , and  $M_{\text{min}}$  which characterize the mass spectrum of the PBHs, while the dashed black horizontal line indicates the  $k$ -independent GW spectrum obtained within the context of the standard cosmology. The gray regions indicated in the upper left portion of each panel indicate the projected discovery reaches of several operating, planned, or proposed experiments capable of probing the GW spectrum within the range of frequencies shown, including LISA [109, 110], the Big Bang Observer (BBO) [111–113], DECIGO [114–116], ultimate DECIGO (u-DECIGO) [114, 117–119], THEIA [120],  $\mu$ -ARES [121], the Advanced LIGO and Advanced VIRGO detectors operating in concert (aLIGO) [122–125], Cosmic Explorer (CE) [126, 127], and the Einstein Telescope (ET) [128, 129].

In interpreting the results shown in Fig. 6, we begin by noting that each of the GW spectra appearing therein consists of four distinct segments with different slopes — segments which correspond to the four different frequency intervals in Eq. (4.17) for which  $f < f_{\text{end}}$ . Each of these segments represents the contribution to  $d\Omega_{\text{GW}}/d\log f$  associated with GW modes which reenter the horizon during a particular cosmological epoch, and the slope of each segment is simply the value of the function  $\xi(w)$  in Eq. (4.14) obtained from the equation-of-state parameter during that epoch. By contrast, the contribution to  $d\Omega_{\text{GW}}/d\log f$  from modes with  $f > f_{\text{end}}$  — modes which never exit the horizon and whose energy density is therefore effectively inflated away — is negligible. Thus, each of the GW spectra shown in Fig. 6 may be considered to have an ultraviolet cutoff at  $f_{\text{end}}$ .

The leftmost segment of each GW spectrum, for which

the slope of  $d\Omega_{\text{GW}}/d\log f$  vanishes, is associated with GW modes with frequencies  $f < f_s$  sufficiently low that they reenter the horizon only after the stasis epoch has concluded. Thus, for  $f < f_s$ , the GW spectra obtained for all values of  $\alpha$ ,  $M_{\text{min}}$ , and  $M_{\text{max}}$  coincide with the flat spectrum obtained within the context of the standard cosmology.

The segment immediately to the right of this first segment corresponds to the frequency interval  $f_s < f < f_{\text{PBH}}$  and is associated with GW modes which reenter the horizon during the stasis epoch itself. The slope  $\xi(\bar{w})$  of this segment depends non-trivially on  $\alpha$  through Eqs. (2.31) and (4.14), as shown in the left panel of the figure. However, for any value of  $\alpha$  within the physically sensible range in Eq. (2.30), it is always the case that  $\xi(w) < 0$ . Since the slope of  $d\Omega_{\text{GW}}/d\log f$  is always negative for  $f_s < f < f_{\text{PBH}}$ , we find that  $d\Omega_{\text{GW}}/d\log f$  is always suppressed within this frequency interval relative to  $d\Omega_{\text{GW}}^{\text{sc}}/d\log f$ . Moreover, while this slope is entirely determined by the value of  $\alpha$ , the frequency  $f_s$  above which this suppression begins depends on the duration of the stasis epoch, and thus on the value of  $M_{\text{max}}$ . Taken together, the solid blue, red, and yellow curves in the right panel of the figure illustrate the effect of varying  $M_{\text{max}}$  with  $\alpha$  and  $M_{\text{min}}$  held fixed. As  $M_{\text{min}}$  increases,  $f_s$  shifts to a lower frequency.

The segment immediately to the right of this second segment corresponds to the frequency interval  $f_{\text{PBH}} < f < f_f$  and is associated with GW modes which reenter the horizon during the epoch of PBH-domination that immediately precedes stasis. Since  $\xi(0) = -2$  and thus  $\xi(0) \leq \xi(\bar{w})$  during this matter-dominated epoch, the downward slope of the GW spectrum steepens — or, in the special case in which  $\bar{w} = 0$ , remains at its stasis value — when  $f$  increases above  $f_{\text{PBH}}$ . The value of this transition frequency depends on the point in the cosmological timeline at which the PBH-domination epoch begins, and thus on the value of  $M_{\text{min}}$ . The solid, dashed, and dotted red curves in the right panel of Fig. 6, taken together, illustrate the effect on the GW spectrum of varying  $M_{\text{min}}$  with  $\alpha$  and  $M_{\text{max}}$  held fixed. As  $M_{\text{min}}$  decreases,  $f_{\text{PBH}}$  shifts to a higher frequency. We also note, however, that the value of  $f_{\text{PBH}}$  depends on  $\alpha$  as well. This is because the rate at which perturbation modes cross the horizon during any particular cosmological epoch depends on  $w$ . Indeed, during any epoch wherein  $w$  is effectively constant, the scale factor scales with time according to the relation  $a \propto t^{2/(3+3w)}$ . It therefore follows from Eq. (4.12) that the relationship between the wavenumber  $k$  of a GW mode which enters the horizon during such an epoch and the time  $t_k$  at which that mode enters the horizon is given by

$$k \sim t_k^{-\frac{(1+3w)}{3(1+w)}}. \quad (4.19)$$

This implies that for a fixed  $\log t_k$  interval, the corresponding  $\log k$  interval — and thus also the corresponding interval of  $\log f$  — increases with increasing  $w$ . As a

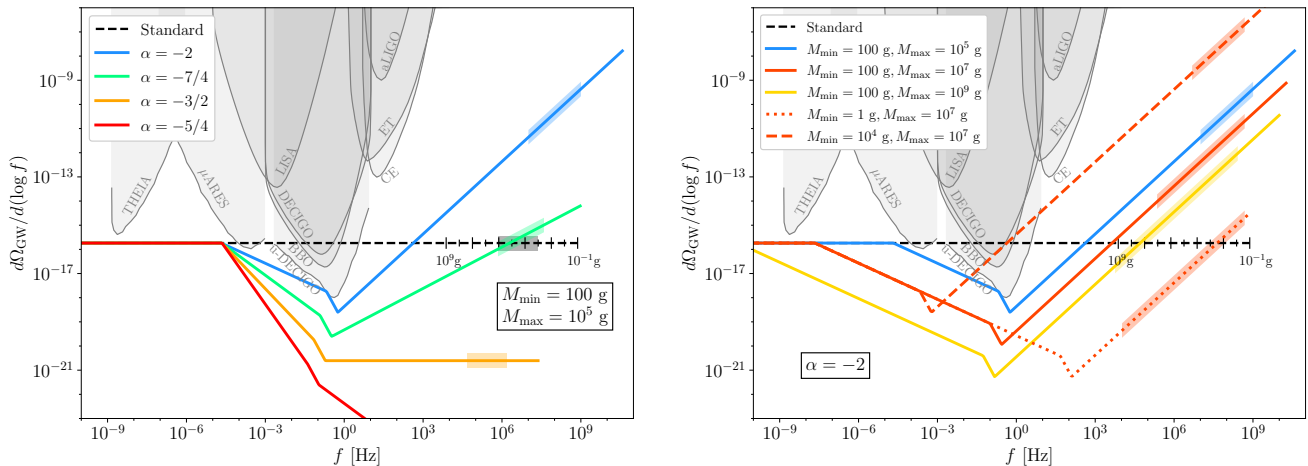


Fig. 6. The GW spectra — *i.e.*, differential abundance of GWs per unit logarithmic present-day GW-frequency  $\log f$  — produced by a scale-invariant spectrum of primordial tensor perturbations in cosmologies involving an epoch of PBH-induced stasis. The colored curves in each panel indicate the GW spectra obtained for different choices of the parameters  $\alpha$ ,  $M_{\min}$ , and  $M_{\max}$  which characterize the mass spectrum of the PBHs, while the dashed black horizontal line indicates the  $k$ -independent GW spectrum obtained within the context of the standard cosmology. In the left panel, we display the GW spectra obtained for several different choices of  $\alpha$  within the physically allowed range in Eq. (2.30) for fixed  $M_{\min} = 100$  g and  $M_{\max} = 10^5$  g. By contrast, in the right panel, we display the GW spectra obtained for several different combinations of  $M_{\min}$  and  $M_{\max}$  for fixed  $\alpha = -2$  (a value of  $\alpha$  which corresponds to  $\bar{w} = 1/5$  and  $w_c = 1$ ). The range of GW frequencies which is associated via Eq. (4.20) with the production of PBHs with masses in the range  $10^{-1}$  g  $< M_i < 10^9$  g within the context of the standard cosmology is indicated by the tick-marks which appear along the right portion of the dashed black line. The range of GW frequencies which is associated with this same range of  $M_i$  within the context of a cosmology involving an epoch of PBH-induced stasis characterized by a particular combination of  $\alpha$ ,  $M_{\min}$ , and  $M_{\max}$  is indicated by the shaded bar which appears along the corresponding  $d\Omega_{\text{GW}}^{\text{sc}}/d\log f$  curve. Since a significant abundance of PBHs is necessary for achieving stasis,  $d\Omega_{\text{GW}}^{\text{sc}}/d\log f$  is expected to receive additional enhancements within this frequency range relative to the result shown here, which pertains to the case of a perfectly scale-invariant spectrum of primordial tensor perturbations.

result, the segment of the GW spectrum associated with modes which reenter the horizon during the stasis epoch spans a larger range of  $\log f$  for smaller  $\alpha$ . This effect, while not particularly dramatic, is evident in the GW spectra shown in the left panel of the Fig. 6.

Finally, the rightmost segment of each spectrum, which corresponds to the frequency interval  $f_f < f < f_{\text{end}}$ , is associated with GW modes which reenter the horizon during the epoch following inflation wherein the population of PBHs is initially produced. Within this frequency interval, the slope  $\xi(w_c)$  of  $d\Omega_{\text{GW}}/d\log f$  can take a broad range of values, depending on the value of  $\alpha$ , as shown in the left panel of Fig. 6. For  $\alpha > -3/2$ , we find that  $\xi(w_c) < 0$ . As a result,  $d\Omega_{\text{GW}}/d\log f$  remains suppressed relative to the result obtained within the context of the standard cosmology, even at high frequencies. The GW spectrum also remains suppressed at high frequencies for  $\alpha = -3/2$ , which corresponds to the special case in which the population of PBHs was produced during a radiation-dominated epoch. In this case,  $\xi(w_c) = 0$  and  $d\Omega_{\text{GW}}/d\log f$  remains flat during this epoch. By contrast, for  $\alpha < -3/2$ , we find that  $\xi(w_c) > 0$ . As a result we find that  $d\Omega_{\text{GW}}/d\log f$  can actually become quite large as  $f$  approaches  $f_{\text{end}}$ . Indeed, for many of the GW spectra shown in Fig. 6,  $d\Omega_{\text{GW}}/d\log f$  is enhanced

relative to  $d\Omega_{\text{GW}}^{\text{sc}}/d\log f$  at high frequencies by several orders of magnitude.

Taken together, the results shown in Fig. 6 indicate that in cosmologies involving a period of PBH-induced stasis, the prospects for observing a stochastic background of gravitational waves can be affected in a variety of ways, depending on the values of  $\alpha$ ,  $M_{\min}$ , and  $M_{\max}$  which characterize the population of PBHs. On the one hand, a suppression of  $d\Omega_{\text{GW}}/d\log f$  at low frequencies — and especially within the frequency range  $10^{-5}$  Hz  $\lesssim f \lesssim 10^2$  Hz for which discovery prospects at future GW detectors are the brightest — could serve to “hide” the SGWB from these detectors. Indeed, this suppression arises due to the stasis epoch itself and to the preceding epoch of PBH domination. On the other hand, the enhancement of  $d\Omega_{\text{GW}}/d\log f$  at high frequencies could potentially enhance the prospects for SGWB discovery. Moreover, since the slope of  $d\Omega_{\text{GW}}/d\log f$  within the interval  $f_s < f < f_{\text{PBH}}$  and the slope of  $d\Omega_{\text{GW}}/d\log f$  within the interval  $f_f < f < f_{\text{end}}$  are both determined solely by the value of  $\alpha$ , the correlation between these two slopes can be exploited as a means of testing whether a particular GW spectrum is potentially the result of an expansion history which includes an epoch of PBH-induced stasis, and even as a means of

indirectly measuring  $\alpha$ .

While modifications to the expansion history of the universe can have a significant impact on  $d\Omega_{\text{GW}}/d\log f$  in cosmologies involving an epoch of PBH-induced stasis, other modifications to the GW spectrum are generically expected in such cosmologies as well. One such modification is linked to the manner in which the population of PBHs is assumed to be produced. The fact that a non-negligible abundance of PBHs arises from the collapse of primordial curvature perturbations in such cosmologies suggests that the amplitude of such perturbations is enhanced on small distance scales. However, small-scale curvature perturbations of this sort generically induce a contribution to the SGWB through their coupling to the tensor perturbations — a coupling which arises at second-order in the perturbed Einstein equations [130–136]. This contribution is therefore an expected feature of the GW spectrum in cosmologies involving an epoch of PBH-induced stasis.

As discussed in Sect. II, the initial mass  $M_i$  of a PBH produced by a perturbation mode with comoving wavenumber  $k$  is correlated with the mass contained within the horizon volume at the time  $t_k$  at which the mode reenters the horizon. Within the context of any particular cosmological model, it then follows that each value of  $M_i$  within the PBH mass spectrum can be associated with a particular value of  $k$ , and hence a particular frequency  $f$ . In the standard cosmology, the relationship between  $M_i$  and  $f$  takes the form (for details, see, *e.g.*, Ref. [137])

$$f \approx (2.4 \times 10^8 \text{ Hz}) \times \gamma^{1/2} \left(\frac{g_\star}{100}\right)^{-1/12} \left(\frac{M_i}{1 \text{ g}}\right)^{-1/2}, \quad (4.20)$$

where  $\gamma$  is the  $\mathcal{O}(1)$  proportionality factor introduced in Eq. (2.1). Thus, for a population of PBHs with masses  $0.1 \text{ g} \lesssim M_i \lesssim 10^9 \text{ g}$  within our regime of interest, the corresponding range of GW frequencies is  $\mathcal{O}(10^3) \text{ Hz} \lesssim f \lesssim \mathcal{O}(10^9) \text{ Hz}$ . This frequency range lies well above the range of  $f$  to which current or future terrestrial or space-based GW interferometers are typically sensitive.

By contrast, in scenarios in which the cosmological history departs from that of the standard cosmology at early times,  $M_i$  and  $f$  are in general not related by Eq. (4.20) [138–141]. In order to determine how these quantities are related in cosmologies involving a PBH-induced epoch of cosmic stasis, we begin by noting that  $H_k$  and  $M_i$  are related through Eq. (2.1) and that

$$a_k = a_s e^{-\mathcal{N}(t_k, t_s)}, \quad (4.21)$$

where the subscript “s” once again indicates the value of a quantity at the end of the stasis epoch and where  $\mathcal{N}(t_k, t_s)$  is the number of  $e$ -folds of expansion that occur between the time at which the mode with wavenumber  $k$  enters the horizon and the end of the stasis epoch. This latter quantity may be expressed as

$$\mathcal{N}(t_k, t_s) = \mathcal{N}_c(t_k) + \mathcal{N}_{\text{PBH}} + \mathcal{N}_s, \quad (4.22)$$

where  $\mathcal{N}_c(t_k)$  denotes the number of  $e$ -folds of expansion that occur between the time at which the mode reenters the horizon and the end of the PBH-formation epoch. Furthermore, the relationship between  $a_s$  and the scale factor  $a_{\text{eq}}$  at matter-radiation equality in the standard cosmology can be derived from the entropy-conservation relation

$$g_\star S(T_s) a_s^3 T_s^3 = g_\star S(T_{\text{eq}}) a_{\text{eq}}^3 T_{\text{eq}}^3, \quad (4.23)$$

where  $g_\star S(T)$  denotes the effective number of entropic degrees of freedom at temperature  $T$ . Thus, approximating the transition from stasis to the radiation-domination epoch as instantaneous, we find that

$$\rho_s = \frac{\pi^2}{30} g_\star(T_s) T_s^4 \approx \frac{3M_P^2 H^2}{8\pi} \approx \frac{M_P^2 \bar{\kappa}^2}{24\pi\tau^2 (M_{\text{max}})}, \quad (4.24)$$

where  $g_\star(T)$  denotes the effective number of relativistic degrees of freedom at temperature  $T$  and where we have defined  $\bar{\kappa} \equiv 2/(1 + \bar{w})$ . Combining these individual relations, we find that the relationship between  $f$  and  $M_i$  in cosmologies involving an epoch of PBH-induced stasis is given by

$$\begin{aligned} f &= \frac{\gamma}{\sqrt{\varepsilon \bar{\kappa}}} \left(\frac{M_{\text{max}}^3}{M_P}\right)^{1/2} \left[\frac{g_\star S(T_{\text{eq}})}{g_\star S(T_s)}\right]^{1/3} \\ &\quad \times \left[\frac{\pi^3 g_\star(T_s)}{180}\right]^{1/4} \frac{a_{\text{eq}} T_{\text{eq}}}{M_i} e^{-\mathcal{N}(t_k, t_s)} \\ &\approx (1.48 \times 10^{10} \text{ Hz}) \times \gamma \left(\frac{2}{\bar{\kappa}}\right)^{1/2} \left(\frac{M_{\text{max}}}{10^9 \text{ g}}\right)^{3/2} \left(\frac{1 \text{ g}}{M_i}\right) \\ &\quad \times \left[\frac{g_\star(T_s)}{10}\right]^{-1/12} e^{40 - \mathcal{N}_c(t_k) - \mathcal{N}_{\text{PBH}} - \mathcal{N}_s} \end{aligned} \quad (4.25)$$

The relationship between  $f$  and  $M_i$  given by Eq. (4.25) can differ significantly from the corresponding result in Eq. (4.20) for the standard cosmology. Indeed, the value of  $f$  which corresponds to a given value of  $M_i$  depends sensitively on the total number of  $e$ -folds that the corresponding perturbation mode experiences during the non-standard part of cosmological history after its horizon reentry.

The range of  $f$  which corresponds to the range  $M_{\text{min}} < M_i < M_{\text{max}}$  of initial PBH masses for each  $d\Omega_{\text{GW}}^{\text{sc}}/d\log f$  curve shown in the figure is indicated by the shaded bar which lies along that curve. The corresponding range of  $f$  obtained for a given range of  $M_i$  within the context of the standard cosmology is demarcated by the tick-marks corresponding to the values of  $M_{\text{max}}$  (on the left) and  $M_{\text{min}}$  (on the right) which appear along the dashed black line in each panel of the figure. Since a significant abundance of PBHs is necessary for achieving stasis,  $d\Omega_{\text{GW}}^{\text{sc}}/d\log f$  is expected to receive additional enhancements within this frequency range.

The results shown in the left panel of Fig. 6 indicate not only that the frequency range corresponding to the range  $M_{\text{min}} < M_i < M_{\text{max}}$  of PBH masses broadens as  $\alpha$



decreases for fixed  $M_{\min}$  and  $M_{\max}$ , but also that this frequency range shifts to larger values of  $f$ . We may account for the latter phenomenon by noting that  $f$  depends on  $\alpha$  primarily through the quantities  $\mathcal{N}_s$  and  $\mathcal{N}_c(t_k)$  which appear in the exponential factor in Eq. (4.25). The first of these quantities decreases with decreasing  $\alpha$  according to Eq. (3.3). The second depends on  $\alpha$  through  $w_c$  according to the relation

$$\mathcal{N}_c(t_k) \approx \frac{2}{3(1+w_c)} \log\left(\frac{t_f}{t_k}\right), \quad (4.26)$$

where  $t_f$  denotes the time at the end of the PBH-formation epoch. Equivalently, through use of Eq. (4.19), we may express  $\mathcal{N}_c(t_k)$  in terms of  $k$  rather than  $t_k$ :

$$\mathcal{N}_c(t_k) \approx \frac{2}{1+3w_c} \log\left(\frac{k_f}{k}\right). \quad (4.27)$$

Since the ratio  $k_f/k$  is independent of  $w_c$  for GWs which enter the horizon during the PBH-formation epoch, Eq. (4.27) indicates that  $\mathcal{N}_c(t_k)$  decreases as  $w_c$  increases. Thus, both  $\mathcal{N}_s$  and  $\mathcal{N}_c(t_k)$  decrease as  $\alpha$  decreases, which accounts for the shift in the frequency range corresponding to  $M_{\min} < M_i < M_{\max}$  to larger values of  $f$ .

In order to account for the broadening of the frequency range which corresponds to the range of PBH masses, we begin by noting that for any two GW modes with frequencies  $f_1$  and  $f_2$  which respectively correspond to a pair of initial PBH masses  $M_1$  and  $M_2$  such that  $M_{\min} \leq M_1 < M_2 \leq M_{\max}$ , Eq. (4.25) implies that

$$\log f_2 - \log f_1 = \log\left(\frac{M_2}{M_1}\right) - \Delta\mathcal{N}_c(t_1, t_2), \quad (4.28)$$

where

$$\Delta\mathcal{N}_c(t_1, t_2) \equiv \mathcal{N}_c(t_2) - \mathcal{N}_c(t_1) \approx \frac{2}{3(1+w_c)} \log\left(\frac{t_2}{t_1}\right) \quad (4.29)$$

represents the number of  $e$ -folds of cosmic expansion which occur between the times at which these modes reenter the horizon. Equivalently, through use of Eq. (2.1), which implies that  $M_i = 3\gamma M_P^2(1+w_c)t_i/4$ , we may express this number of  $e$ -folds in terms of  $M_1$  and  $M_2$  directly:

$$\Delta\mathcal{N}_c(t_1, t_2) \approx \frac{2}{3(1+w_c)} \log\left(\frac{M_2}{M_1}\right). \quad (4.30)$$

We see from this relation that as  $w_c$  increases,  $\Delta\mathcal{N}_c(t_1, t_2)$  decreases and the corresponding logarithmic frequency interval in Eq. (4.28) increases. Identifying  $M_1$  and  $M_2$  with  $M_{\min}$  and  $M_{\max}$ , we then observe that the range of frequencies within which we expect  $d\Omega_{\text{GW}}/d\log f$  to be enhanced due to the physics underlying the formation of PBHs in cosmologies involving an epoch of PBH-induced stasis indeed broadens as  $\alpha$  decreases.

Overall, for typical parameter values, the corresponding GW frequency ranges from MHz to GHz, still much

higher than what the space-based or terrestrial interferometer can reach. However, the SGWB could potentially be probed within this frequency range by experiments designed primarily to detect axion dark matter [142–146]. We leave investigations along these lines for future work.

Finally, in addition to the contributions to the GW spectrum discussed above, there is an additional contribution which arises in cosmologies involving an epoch of PBH-induced stasis due to the presence of the PBHs themselves. Since PBHs are discrete objects, their spatial distribution is granular on small scales and is therefore not strictly adiabatic. As a result, density perturbations associated with a population of PBHs necessarily include an isocurvature component [147]. These isocurvature perturbations can be converted into adiabatic curvature perturbations during a PBH-dominated epoch [148, 149], and therefore act as an additional source for GW production [139, 150–157]. These processes are generically active during any cosmological epoch wherein PBHs constitute a non-negligible fraction of the total energy density of the universe. In cosmologies involving an epoch of PBH-induced stasis, one would therefore expect these processes to be active both during the stasis epoch itself and during the PBH-dominated epoch which immediately precedes it. Thus, one would generically expect an additional contribution to the GW spectrum to arise as a result of this isocurvature contribution in such cosmologies. We leave the analysis of this contribution for future work.

#### D. Dark Radiation

In extensions of the SM involving one or more additional light particle species — *e.g.*, axions, axion-like particles, dark photons, sterile neutrinos, and gravitons — particles of these species are generically produced as Hawking radiation. The evaporation of a population of PBHs can therefore generate a potentially sizable contribution to the abundance of dark radiation. This dark radiation could potentially manifest itself at future CMB observatories as a shift  $\Delta N_{\text{eff}}$  in the effective number of light neutrino species  $N_{\text{eff}}$  present in the early universe (for recent reviews, see, *e.g.*, Ref. [158] and references therein). Particular attention has been focused on the contribution to  $\Delta N_{\text{eff}}$  which arises from the evaporation of a population of Kerr PBHs, since rapidly rotating BHs are expected to produce higher-spin particles more efficiently than non-rotating ones [9, 10, 16, 17, 24, 159–162]. The contribution to  $\Delta N_{\text{eff}}$  which arises from a population of PBHs with an extended distribution of both masses and spins was recently investigated in Ref. [163]. Here, we investigate the effect that an epoch of cosmic stasis has on  $\Delta N_{\text{eff}}$ .

In Fig. 7, we plot the contribution to  $\Delta N_{\text{eff}}$  that arises from the production of additional, light degrees of freedom via PBH evaporation as a function of  $M_{\max}$  in a modified cosmology involving a stasis epoch. The solid

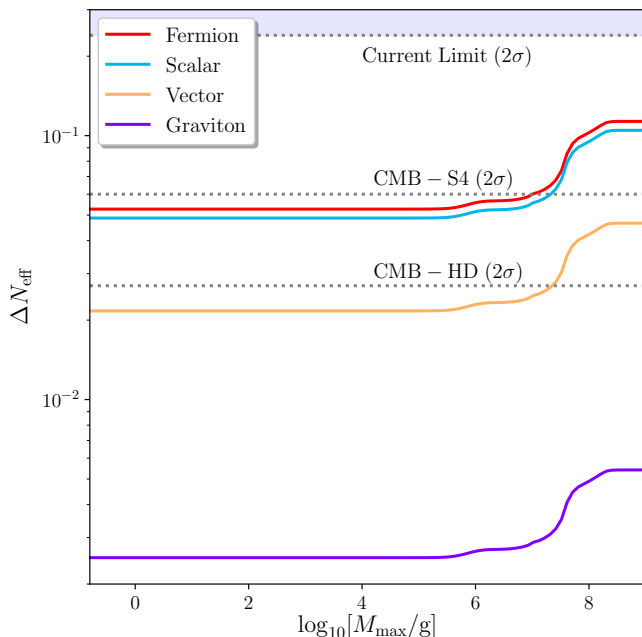


Fig. 7. Contributions to  $\Delta N_{\text{eff}}$  from the evaporation of a population of PBHs with a power-law distribution of masses into dark radiation in SM extensions involving a single additional light particle species, plotted as functions of  $\log_{10}(M_{\text{max}}/\text{g})$ . The solid curves correspond to different representations of the Lorentz group under which particles of that species transform. All such curves correspond to the parameter choices  $M_{\text{min}} = 0.1 \text{ g}$  and  $\alpha = -1$ ; however, the value of  $\Delta N_{\text{eff}}$  is insensitive to both  $M_{\text{min}}$  and  $\alpha$ . The shaded region above the uppermost dashed line is excluded by current bounds at the  $2\sigma$  significance level. The additional dashed lines indicate the reach of future CMB experiments, as represented by the corresponding projected  $2\sigma$  limits.

curves indicate the  $\Delta N_{\text{eff}}$  contribution associated with various particle species that arise in different extensions of the SM. The red curve represents the contribution from a gauge-singlet Majorana fermion. The cyan curve represents the contribution from a real Lorentz scalar field. The orange curve represents the contribution from a massless Lorentz vector, and the purple curve represents the contribution from a massless graviton. These curves correspond to the parameter choices  $M_{\text{min}} = 0.1 \text{ g}$  and  $\alpha = -1$ ; however, we find that the value of  $\Delta N_{\text{eff}}$  is essentially insensitive to both  $M_{\text{min}}$  and  $\alpha$ . The shaded region above the uppermost dashed line is excluded by current bounds on  $\Delta N_{\text{eff}}$  at the  $2\sigma$  significance level. The additional dashed lines represent the projected  $2\sigma$  limits on  $\Delta N_{\text{eff}}$  which would be provided by the CMB-S4 [105, 164] and CMB-HD [165] experiments in the event of a non-detection — limits which provide an indication of the discovery reach of these future experiments.

The results shown in Fig. 7 indicate that current bounds on  $\Delta N_{\text{eff}}$  do not exclude the presence of a single additional species of light, SM-gauge-singlet particle beyond the particle content of the SM in cosmologies involv-

ing an epoch of PBH-induced stasis. However, depending on the properties of this additional particle species, future CMB experiments could be potentially be sensitive to the shift in  $N_{\text{eff}}$  which results from the production of these particles via Hawking radiation. We also observe that  $\Delta N_{\text{eff}}$  is effectively independent of  $M_{\text{max}}$  when  $M_{\text{max}}$  is small, but depends non-trivially on  $M_{\text{max}}$  when  $M_{\text{max}} \gtrsim 10^5 \text{ g}$ . This dependence of  $\Delta N_{\text{eff}}$  on  $M_{\text{max}}$  is due to the lifetime  $\tau(M_{\text{max}})$  of the heaviest PBHs being sufficiently long in this regime that the electroweak phase-transition occurs during the stasis epoch. Once this phase transition occurs, the effective number of relativistic degrees of freedom  $g_*(T)$  in the radiation bath begins to depend non-trivially on  $T$  — and hence on time. Thus, for  $M_{\text{max}} \gtrsim 10^5 \text{ g}$ , the production of light particles via Hawking radiation remains significant after the electroweak phase transition has occurred — and for  $M_{\text{max}} \gtrsim 10^7 \text{ g}$ , even after the quark-hadron phase transition has occurred — and  $g_*(T)$  has fallen below its initial high-temperature value. The contribution to  $\Delta N_{\text{eff}}$  from such a long-lived population of PBHs is therefore greater than the contribution from a population of short-lived PBHs which all decay before the electroweak phase transition occurs.

It is also noteworthy that these results depend neither on the value of the parameter  $\alpha$  nor on the value of the initial mass  $M_{\text{min}}$ . Indeed, across the full range of  $M_i$  relevant for stasis, the corresponding initial Hawking temperature  $T_{\text{BH}} = M_P^2/(8\pi M_i)$  is sufficiently large that all SM degrees of freedom may be considered relativistic when they are produced via the evaporation of even the lightest PBHs. As a result, the ratio of the energy density of dark radiation generated by PBH evaporation to the energy density of SM particles generated in this way remains effectively constant across the time period during which the PBHs are evaporating. The total contribution to the energy density of dark radiation at times after the end of the stasis epoch therefore depends effectively only on  $\tau(M_{\text{max}})$ .

## E. Dark Matter

In a similar vein, it is also interesting to consider possible connections between the PBHs which give rise to cosmic stasis in cosmologies of this sort and the dark matter (DM) which overwhelming evidence suggests constitutes a significant fraction of the present-day energy density of the universe. The PBHs which give rise to the epoch of PBH-induced cosmic stasis evaporate far too rapidly to contribute to the present-day abundance of DM themselves. By contrast, longer-lived PBHs produced by the collapse of lower-frequency perturbations could of course in principle contribute to this abundance (see, *e.g.*, Ref. [3] for a recent review), but such PBHs are not a necessary ingredient in cosmologies involving PBH-induced stasis. Nevertheless, even though the PBHs which give rise to the stasis epoch cannot themselves con-

tribute to the present-day DM abundance, their evaporation can play an important role in producing particles that *do* constitute the DM. Indeed, DM particles are generically expected to be produced as Hawking radiation as PBHs evaporate, just as SM particles are [166].

The effect of this production mechanism on the present-day DM abundance has been investigated both for the case of a monochromatic PBH mass spectrum [9–12, 16, 19, 20, 26, 28, 30, 167, 168] and for the case of an extended PBH mass spectrum, including one with the power-law profile we consider here [163]. In the latter case, it was shown that for  $\mathcal{O}(\text{GeV})$  DM candidates, the broader the PBH distribution is, the smaller the initial abundance of PBHs must be and the shorter their lifetimes must be in order to guarantee that DM is not overproduced.

Considerations related to small-scale structure place additional constraints on the population of DM particles generated by PBH evaporation. If a non-negligible fraction of these particles are produced by PBHs with Hawking temperatures  $T_{\text{PBH}} \gg m_{\text{DM}}$ , the resulting contribution to the DM phase-space distribution will be highly relativistic. If the DM is effectively decoupled from the thermal bath by the time this contribution arises, the free-streaming effects associated with such a population of “hot” DM particles can suppress the formation of structure on small scales. Lyman- $\alpha$ -forest data [169–175] imply stringent constraints on such a “hot” population of DM particles. Indeed, scenarios in which a population of PBHs with an extended mass spectrum comes to represent a significant fraction of the energy density of universe by the time those PBHs evaporate are typically excluded by these constraints if the DM particles are light — in the sense that  $m_{\text{DM}} \ll M_{\text{P}}^2/(8\pi M_{\text{max}})$  — and effectively decoupled [163]. Since PBHs collectively contribute an  $\mathcal{O}(1)$  fraction of the total energy density in cosmologies involving a PBH-induced stasis epoch, small-scale-structure constraints are a serious concern.

One way of circumventing these overclosure and structure-formation constraints is simply to posit that the DM particles interact sufficiently strongly with the particles in the radiation bath that they remain in thermal equilibrium with those particles until well after the last PBHs evaporate and the stasis epoch ends. In this case, the DM particles produced via Hawking radiation rapidly thermalize and an acceptable present-day DM abundance can be generated, *e.g.*, through thermal freeze-out.

However, another possible way of circumventing these constraints — one in which the evaporation of the PBHs which give rise to stasis indeed *does* serve as an important mechanism for DM production — is to posit that the masses of the particles which constitute the DM today significantly exceeds the initial Hawking temperature of even the lightest PBHs — *i.e.*, that  $m_{\text{DM}} \gg M_{\text{P}}^2/(8\pi M_{\text{min}})$ . Indeed, the production of such DM particles with such masses due to the evaporation of PBHs with any initial mass  $M_{\text{min}} < M_i < M_{\text{max}}$  remains highly

Boltzmann-suppressed until those PBHs lose the vast majority of their initial mass. Provided that  $m_{\text{DM}}$  is sufficiently large, the resulting population of DM particles will not dominate the energy of the universe prematurely.

Moreover, structure-formation constraints on the DM phase-space distribution are less of a concern when  $m_{\text{DM}} \gg M_{\text{P}}^2/(8\pi M_{\text{min}})$ . There are two principal reasons for this. The first is that the majority of the DM particles in this population are produced by PBHs whose Hawking temperatures have only just crossed the threshold  $T_{\text{BH}} \sim m_{\text{DM}}$  above which DM production is no longer Boltzmann-suppressed. As a result, most of the DM particles produced via PBH evaporation are not highly relativistic even at the time at which they are initially produced. The second is that for values of  $\alpha$  within the range specified in Eq. (2.30), PBHs with smaller  $M_i$  contribute a greater portion of the total initial PBH energy density. These lighter PBHs evaporate comparatively early during the stasis epoch, and the momenta of the DM particles that they produce are therefore redshifted to a greater extent by the end of the stasis epoch than are the DM particles produced at the end of that epoch via the evaporation of heavier PBHs. Thus, while lighter PBHs lose a smaller fraction of their initial mass energy before they are capable of producing DM particles, this is compensated for by this redshifting effect. Indeed, it is known that for the case of a monochromatic initial PBH spectrum in which all of the PBHs have  $M_i = 10^6 \text{ g}$ , both the overclosure bound and the Lyman- $\alpha$  constraints on the DM phase-space distribution can be satisfied for  $m_{\text{DM}} \geq 10^{16} \text{ GeV}$  [19].

In light of these considerations, it is therefore conceivable that Hawking radiation could serve as the dominant mechanism for DM production in cosmologies involving an epoch of PBH-induced stasis, provided that  $m_{\text{DM}}$  lies only a couple of orders of magnitude below the Planck scale. That said, obtaining a reliable lower bound on  $m_{\text{DM}}$  for a given combination of  $\alpha$ ,  $M_{\text{min}}$  and  $M_{\text{max}}$  in cosmologies of this sort is challenging for two reasons. The first of these is that the quantity  $\epsilon(M)$  in Eq. (2.7) depends non-trivially on  $M$  in this case through the gray-body factor. The second is that DM particles with such large values of  $m_{\text{DM}}$  are only produced via the evaporation of a PBH with initial mass  $M_i$  during an extremely brief time interval around  $t \sim \tau(M_i)$ . An accurate assessment of the contributions to the DM abundance and phase-space distribution from PBH evaporation therefore requires a high degree of precision — a degree of precision beyond what numerical tools such as FRISBHEE provide. We leave the dedicated analysis that would be required in order to determine the lower bound on  $m_{\text{DM}}$  in cosmologies with PBH-induced stasis for future work.

We also remark that the dark matter may not consist of particles of a single mass  $m_{\text{DM}}$ . Indeed, there exist frameworks for DM physics — most notably the Dynamical Dark Matter (DDM) framework [176–178] — wherein the particles which constitute the DM exhibit both an extended mass spectrum and a non-trivial spectrum of

abundances, not unlike the PBHs we consider here. The connection between PBHs and DM within these frameworks is likely to involve a rich and complicated dynamics which might, for example, enforce correlations between the PBH scaling exponent  $\alpha$  and the scaling exponents and other parameters which govern the manner in which the abundances, lifetimes, *etc.*, of the DM states scale as a function of their mass. This too represents an interesting direction for further study.

## F. Baryogenesis

PBH-induced stasis can have potentially significant implications for baryogenesis as well. Given the allowed range of PBH masses in Eq. (2.5), it is in principle possible for the temperature of the radiation bath during stasis to span a range of temperatures ranging from just above the BBN scale (*i.e.*, a few MeV) up to around  $10^{11}$  GeV. The modification of the expansion history of the universe across such a broad range of energy scales can impact baryogenesis in a number of ways.

For example, the possibility that the electroweak phase transition could take place during the stasis epoch has implications for electroweak baryogenesis. Indeed, in scenarios in which the universe expands more rapidly during the electroweak phase transition than it does in the standard cosmology, the degree to which the baryon asymmetry is washed out by sphaleron processes is diminished [179–182]. In baryogenesis scenarios in which the baryon asymmetry of the universe is instead ultimately generated via the out-of-equilibrium decays of heavy particles with  $CP$ -violating interactions — including scenarios which achieve baryogenesis through leptogenesis — it is possible that these decays could occur during the stasis epoch. In leptogenesis scenarios involving right-handed neutrinos (RHN) with masses  $M_N \sim \mathcal{O}(10^9 - 10^{10})$  GeV, for example, the thermal RHN population which is initially in equilibrium with the radiation bath can potentially decay during the stasis epoch, provided that  $M_{\min}$  is sufficiently small. The rates for inverse-decay processes and for other processes which serve to wash out the lepton asymmetry generated by RHN decays would therefore be modified in these scenarios relative to the rates obtained in the context of the standard cosmology.

Furthermore, in scenarios in which the baryon asymmetry is generated by the out-of-equilibrium decays of heavy particles, there is an additional effect which can significantly impact this asymmetry in cosmologies involving an epoch of PBH-induced stasis. This is that these heavy particles can be produced via the evaporation of the PBHs themselves. Indeed, even if these particles are sufficiently massive that they are not produced by the thermal bath during the stasis epoch, they could nevertheless be produced as Hawking radiation.

The contribution to the baryon asymmetry of the universe which results from the production of heavy,  $CP$ -violating particles as Hawking radiation was considered

in Refs. [18, 26, 33–36, 60, 168, 183–189] for the case of a monochromatic PBH mass spectrum. On the one hand, the effect of entropy dilution from PBH decay renders it challenging to obtain a sufficient baryon asymmetry, *e.g.*, in Majorana leptogenesis scenarios in which  $10^6 \text{ GeV} \lesssim M_N \lesssim 10^8 \text{ GeV}$  [18, 35]. On the other hand, since the interaction rates associated with lepton-number-violating washout processes involving particles in the thermal bath are suppressed at low temperatures, the contribution to the baryon asymmetry from RHN produced at late times from PBH evaporation is impacted far less by such processes than the contribution from the decay of a thermal population of RHN [189]. As a result, leptogenesis scenarios in which  $M_N \gtrsim 10^{15} \text{ GeV}$ , which would not yield a sufficient baryon asymmetry within the context for the standard cosmology, can become viable if RHN production from PBH evaporation is significant.

Both the dynamics of particle production from PBH evaporation and entropy generation in cosmologies involving an extended mass spectrum and a protracted period of stasis can differ drastically from the corresponding dynamics in the cosmologies considered in these studies. Thus, assessing the effect of a PBH-induced stasis epoch on the baryon asymmetry in baryogenesis scenarios of this sort would require a dedicated analysis, which we leave for future work.

## V. CONCLUSIONS

A population of PBHs with a mass spectrum of the sort that arises naturally in a variety of cosmological scenarios can give rise to *cosmic stasis* — *i.e.*, an extended period during which multiple cosmological components with different equations of state (in this case, black holes and radiation) have relative abundances that remain effectively constant even as the universe expands. For example, the spectrum of PBHs generated by the collapse of density fluctuations with a scale-invariant power spectrum generically gives rise to stasis, provided that this collapse occurs during an epoch wherein the effective equation-of-state parameter for the universe lies within the range  $0 \leq w_c \leq 1$ . This is in large part due to the fact that stasis is a global attractor for the dynamical system that governs the evolution of the cosmological abundances of matter — *i.e.*, the PBHs — and radiation. Moreover, even though stasis is a global attractor, it is not eternal — indeed, it terminates when the heaviest PBHs evaporate. Thus, since a period of PBH-induced stasis has not only a beginning but also an end, it constitutes a true cosmological epoch. Such a stasis epoch is therefore expected to be a common feature in the cosmological timeline in scenarios involving PBHs with such a spectrum. It is therefore crucial to understand the consequences of such an epoch.

In this paper, we have investigated the phenomenological implications of a PBH-induced stasis epoch. We have shown that this epoch can represent a significant

number of  $e$ -folds of cosmic expansion and span a range of energy scales ranging from  $T \sim 10^{11}$  GeV down to just above the BBN scale. As a result, the modification of the expansion history associated with cosmologies of this sort can have a significant impact on a number of astrophysical observables. We have found, for example, that these modifications can have a significant impact on the values of the spectral tilt  $n_s$  and tensor-to-scalar ratio  $r$  of the primordial perturbation spectrum obtained from CMB data. Moreover, we have also found that these modifications can have a highly non-trivial impact on the stochastic background of GWs which arises from primordial perturbations after inflation. In particular, we have shown that the resulting GW spectrum can be modified in a variety of ways within the frequency range most relevant for detection at future GW-interferometry experiments, depending on the values of the parameters  $\alpha$ ,  $M_{\min}$ , and  $M_{\max}$  which characterize the mass spectrum of the PBHs. However, we have also shown that the scaling behaviors which the GW spectrum exhibits within different frequency intervals are correlated in cosmologies of this sort. These correlations therefore not only provide an observational handle that can be used to verify whether or not a particular SGWB spectrum is consistent with a cosmology involving an epoch of PBH stasis, but also provide information about the values of  $\alpha$ ,  $M_{\min}$ , and  $M_{\max}$  themselves.

We have also considered several additional phenomenological consequences of a PBH-induced stasis epoch in the context of new-physics scenarios which involve additional particle species beyond the particle content of the SM. In particular, we have investigated the shift  $\Delta N_{\text{eff}}$  in the effective number of light neutrino species which arises due to the production of particles which behave as dark radiation via PBH evaporation in cosmologies of this sort. We have shown that the contribution to  $\Delta N_{\text{eff}}$  from a single species of dark-radiation particle is typically consistent with current observational bounds, but also that future CMB experiments could potentially be sensitive to this contribution, especially if  $M_{\max} \gtrsim 10^7$  g. Moreover, we have also discussed the potential consequences of particle-production via Hawking radiation during a PBH-induced stasis epoch for baryogenesis and for the production of DM. In doing so, we have highlighted the particular ways in which the presence of the stasis epoch can play a potentially important role in determining the values of quantities such as the baryon asymmetry of the universe and the present-day DM abundance obtained for any particular new-physics scenario.

In closing, we note that another potentially observable consequence of cosmic stasis stems from the fact that density perturbations evolve differently in cosmologies involving a stasis epoch than they do in the standard cosmology. This is due not only to the modification of the expansion history, but also to the fact that when energy density is transferred from matter to radiation — *e.g.*, via the decays of PBHs — perturbations in the energy density of matter serve as a source for perturbations in

the energy density of radiation. Both of these effects are present in cosmologies involving an epoch of early matter domination as well, where they can modify the spectrum of perturbations in the radiation density. In scenarios in which the particle species which will eventually come to constitute the dark matter are still relativistic and in equilibrium with the radiation bath throughout the stasis epoch, this modification can in turn lead to a modification of the shape of the matter power spectrum [190–192]. One would therefore expect similar modifications of the matter power spectrum to arise in cosmologies involving a stasis epoch.

## ACKNOWLEDGEMENTS

The research activities of KRD are supported in part by the U.S. Department of Energy under Grant DE-FG02-13ER41976 / DE-SC0009913 and by the U.S. National Science Foundation through its employee IR/D program. The work of LH is funded by the UK Science and Technology Facilities Council (STFC) under Grant ST/P001246/1. LH also acknowledges the support of the Institut Pascal at Université Paris-Saclay during the Paris-Saclay Astroparticle Symposium 2022, with the support of the IN2P3 master projet UCMN, the P2IO Laboratory of Excellence (program “Investissements d’avenir” ANR-11-IDEX-0003-01 Paris-Saclay and ANR-10-LABX-0038), the P2I axis of the Graduate School Physics of Université Paris-Saclay, as well as IJ-CLab, CEA, IPhT, APPEC, and ANR-11-IDEX-0003-01 Paris-Saclay and ANR-10-LABX-0038. The work of FH and TMPT is supported in part by the U.S. National Science Foundation under Grant PHY-1915005, while the work of FH is also supported in part by the International Postdoctoral Exchange Fellowship Program and the work of TMPT is also supported in part by the U.S. National Science Foundation under Grant PHY-2210283. The work of DK is supported by the U.S. Department of Energy Grant DE-SC0010813. The research activities of BT are supported in part by the U.S. National Science Foundation under Grant PHY-2014104. The opinions and conclusions expressed herein are those of the authors and do not represent any funding agencies.

- 
- [1] S. W. Hawking, *Nature* **248**, 30 (1974).
- [2] S. W. Hawking, *Commun. Math. Phys.* **43**, 199 (1975), [Erratum: *Commun. Math. Phys.* **46**, 206 (1976)].
- [3] A. Escrivà, F. Kuhnel, and Y. Tada, (2022), [arXiv:2211.05767 \[astro-ph.CO\]](#).
- [4] B. Carr, K. Kohri, Y. Sendouda, and J. Yokoyama, (2020), [arXiv:2002.12778 \[astro-ph.CO\]](#).
- [5] A. M. Green and B. J. Kavanagh, *J. Phys. G* **48**, 4 (2021), [arXiv:2007.10722 \[astro-ph.CO\]](#).
- [6] P. Villanueva-Domingo, O. Mena, and S. Palomares-Ruiz, *Front. Astron. Space Sci.* **8**, 87 (2021), [arXiv:2103.12087 \[astro-ph.CO\]](#).
- [7] B. J. Carr, K. Kohri, Y. Sendouda, and J. Yokoyama, *Phys. Rev. D* **81**, 104019 (2010), [arXiv:0912.5297 \[astro-ph.CO\]](#).
- [8] C. Keith, D. Hooper, N. Blinov, and S. D. McDermott, (2020), [arXiv:2006.03608 \[astro-ph.CO\]](#).
- [9] D. Hooper, G. Krnjaic, and S. D. McDermott, *JHEP* **08**, 001 (2019), [arXiv:1905.01301 \[hep-ph\]](#).
- [10] I. Masina, *Eur. Phys. J. Plus* **135**, 552 (2020), [arXiv:2004.04740 \[hep-ph\]](#).
- [11] I. Baldes, Q. Decant, D. C. Hooper, and L. Lopez-Honorez, *JCAP* **08**, 045 (2020), [arXiv:2004.14773 \[astro-ph.CO\]](#).
- [12] P. Gondolo, P. Sandick, and B. Shams Es Haghi, *Phys. Rev. D* **102**, 095018 (2020), [arXiv:2009.02424 \[hep-ph\]](#).
- [13] N. Bernal and O. Zapata, *JCAP* **03**, 007 (2021), [arXiv:2010.09725 \[hep-ph\]](#).
- [14] N. Bernal and O. Zapata, *Phys. Lett. B* **815**, 136129 (2021), [arXiv:2011.02510 \[hep-ph\]](#).
- [15] N. Bernal and O. Zapata, *JCAP* **03**, 015 (2021), [arXiv:2011.12306 \[astro-ph.CO\]](#).
- [16] I. Masina, (2021), [arXiv:2103.13825 \[gr-qc\]](#).
- [17] A. Arbey, J. Auffinger, P. Sandick, B. Shams Es Haghi, and K. Sinha, (2021), [arXiv:2104.04051 \[astro-ph.CO\]](#).
- [18] S. Jyoti Das, D. Mahanta, and D. Borah, (2021), [arXiv:2104.14496 \[hep-ph\]](#).
- [19] A. Cheek, L. Heurtier, Y. F. Perez-Gonzalez, and J. Turner, *Phys. Rev. D* **105**, 015022 (2022), [arXiv:2107.00013 \[hep-ph\]](#).
- [20] A. Cheek, L. Heurtier, Y. F. Perez-Gonzalez, and J. Turner, *Phys. Rev. D* **105**, 015023 (2022), [arXiv:2107.00016 \[hep-ph\]](#).
- [21] P. Sandick, B. S. Es Haghi, and K. Sinha, *Phys. Rev. D* **104**, 083523 (2021), [arXiv:2108.08329 \[astro-ph.CO\]](#).
- [22] F. Schiavone, D. Montanino, A. Mirizzi, and F. Capozzi, *JCAP* **08**, 063 (2021), [arXiv:2107.03420 \[hep-ph\]](#).
- [23] N. Bernal, F. Hajkarim, and Y. Xu, *Phys. Rev. D* **104**, 075007 (2021), [arXiv:2107.13575 \[hep-ph\]](#).
- [24] A. Cheek, L. Heurtier, Y. F. Perez-Gonzalez, and J. Turner, *Phys. Rev. D* **106**, 103012 (2022), [arXiv:2207.09462 \[astro-ph.CO\]](#).
- [25] N. Bernal, Y. F. Perez-Gonzalez, and Y. Xu, *Phys. Rev. D* **106**, 015020 (2022), [arXiv:2205.11522 \[hep-ph\]](#).
- [26] L. Morrison, S. Profumo, and Y. Yu, *JCAP* **1905**, 005 (2019), [arXiv:1812.10606 \[astro-ph.CO\]](#).
- [27] J. Auffinger, I. Masina, and G. Orlando, *Eur. Phys. J. Plus* **136**, 261 (2021), [arXiv:2012.09867 \[hep-ph\]](#).
- [28] M. Y. Khlopov, A. Barrau, and J. Grain, *Class. Quant. Grav.* **23**, 1875 (2006), [arXiv:astro-ph/0406621](#).
- [29] R. Allahverdi, J. Dent, and J. Osinski, *Phys. Rev.* **D97**, 055013 (2018), [arXiv:1711.10511 \[astro-ph.CO\]](#).
- [30] O. Lennon, J. March-Russell, R. Petrossian-Byrne, and H. Tillim, *JCAP* **1804**, 009 (2018), [arXiv:1712.07664 \[hep-ph\]](#).
- [31] T. Kitabayashi, (2021), [arXiv:2101.01921 \[hep-ph\]](#).
- [32] J. D. Barrow, E. J. Copeland, E. W. Kolb, and A. R. Liddle, *Phys. Rev. D* **43**, 984 (1991).
- [33] Y. Hamada and S. Iso, *PTEP* **2017**, 033B02 (2017), [arXiv:1610.02586 \[hep-ph\]](#).
- [34] D. Hooper and G. Krnjaic, *Phys. Rev. D* **103**, 043504 (2021), [arXiv:2010.01134 \[hep-ph\]](#).
- [35] Y. F. Perez-Gonzalez and J. Turner, (2020), [arXiv:2010.03565 \[hep-ph\]](#).
- [36] S. Datta, A. Ghosal, and R. Samanta, (2020), [arXiv:2012.14981 \[hep-ph\]](#).
- [37] N. Bernal, Y. F. Perez-Gonzalez, Y. Xu, and O. Zapata, *Phys. Rev. D* **104**, 123536 (2021), [arXiv:2110.04312 \[hep-ph\]](#).
- [38] J. D. Barrow, E. J. Copeland, and A. R. Liddle, *Mon. Not. Roy. Astron. Soc.* **253**, 675 (1991).
- [39] K. R. Dienes, L. Heurtier, F. Huang, D. Kim, T. M. P. Tait, and B. Thomas, *Phys. Rev. D* **105**, 023530 (2022), [arXiv:2111.04753 \[astro-ph.CO\]](#).
- [40] C. T. Byrnes and P. S. Cole (2021) [arXiv:2112.05716 \[astro-ph.CO\]](#).
- [41] B. Carr and F. Kuhnel, *Ann. Rev. Nucl. Part. Sci.* **70**, 355 (2020), [arXiv:2006.02838 \[astro-ph.CO\]](#).
- [42] B. J. Carr, *Astrophys. J.* **201**, 1 (1975).
- [43] S. Clesse and J. García-Bellido, *Phys. Rev. D* **92**, 023524 (2015), [arXiv:1501.07565 \[astro-ph.CO\]](#).
- [44] A. Dolgov and J. Silk, *Phys. Rev. D* **47**, 4244 (1993).
- [45] A. M. Green, *Phys. Rev. D* **94**, 063530 (2016), [arXiv:1609.01143 \[astro-ph.CO\]](#).
- [46] B. J. Carr and J. E. Lidsey, *Phys. Rev. D* **48**, 543 (1993).
- [47] P. Ivanov, P. Naselsky, and I. Novikov, *Phys. Rev. D* **50**, 7173 (1994).
- [48] J. Garcia-Bellido, A. D. Linde, and D. Wands, *Phys. Rev. D* **54**, 6040 (1996), [arXiv:astro-ph/9605094](#).
- [49] L. Randall, M. Soljaic, and A. H. Guth, *Nucl. Phys. B* **472**, 377 (1996), [arXiv:hep-ph/9512439](#).
- [50] L. Heurtier, A. Moursy, and L. Wacquez, (2022), [arXiv:2207.11502 \[hep-th\]](#).
- [51] K. Dimopoulos, *Phys. Lett. B* **775**, 262 (2017), [arXiv:1707.05644 \[hep-ph\]](#).
- [52] G. Ballesteros and M. Taoso, *Phys. Rev. D* **97**, 023501 (2018), [arXiv:1709.05565 \[hep-ph\]](#).
- [53] A. Karam, N. Koivunen, E. Tomberg, V. Vaskonen, and H. Veermäe, (2022), [arXiv:2205.13540 \[astro-ph.CO\]](#).
- [54] I. Dalianis, A. Kehagias, and G. Tringas, *JCAP* **01**, 037 (2019), [arXiv:1805.09483 \[astro-ph.CO\]](#).
- [55] K. Kannike, L. Marzola, M. Raidal, and H. Veermäe, *JCAP* **09**, 020 (2017), [arXiv:1705.06225 \[astro-ph.CO\]](#).
- [56] M. Crawford and D. N. Schramm, *Nature* **298**, 538 (1982).
- [57] K. Jedamzik, *Phys. Rev. D* **55**, 5871 (1997), [arXiv:astro-ph/9605152](#).
- [58] C. Schmid, D. J. Schwarz, and P. Widerin, *Phys. Rev. D* **59**, 043517 (1999), [arXiv:astro-ph/9807257](#).
- [59] P. Widerin and C. Schmid, (1998), [arXiv:astro-ph/9808142](#).

- [60] S. W. Hawking, I. G. Moss, and J. M. Stewart, *Phys. Rev. D* **26**, 2681 (1982).
- [61] H. Kodama, M. Sasaki, and K. Sato, *Prog. Theor. Phys.* **68**, 1979 (1982).
- [62] S. M. Leach, I. J. Grivell, and A. R. Liddle, *Phys. Rev. D* **62**, 043516 (2000), [arXiv:astro-ph/0004296](#).
- [63] I. G. Moss, *Phys. Rev. D* **50**, 676 (1994).
- [64] N. Kitajima and F. Takahashi, *JCAP* **11**, 060 (2020), [arXiv:2006.13137 \[hep-ph\]](#).
- [65] H. Kodama, M. Sasaki, K. Sato, and K.-i. Maeda, *Prog. Theor. Phys.* **66**, 2052 (1981).
- [66] K.-i. Maeda, *Class. Quant. Grav.* **3**, 651 (1986).
- [67] M. Y. Khlopov, R. V. Konoplich, S. G. Rubin, and A. S. Sakharov, (1998), [arXiv:hep-ph/9807343](#).
- [68] R. V. Konoplich, S. G. Rubin, A. S. Sakharov, and M. Y. Khlopov, *Phys. Atom. Nucl.* **62**, 1593 (1999).
- [69] M. Pavsic, *Grav. Cosmol.* **2**, 1 (1996), [arXiv:gr-qc/9511020](#).
- [70] M. Y. Khlopov, R. V. Konoplich, S. G. Rubin, and A. S. Sakharov, *Grav. Cosmol.* **6**, 153 (2000).
- [71] V. Dokuchaev, Y. Eroshenko, and S. Rubin, *Grav. Cosmol.* **11**, 99 (2005), [arXiv:astro-ph/0412418](#).
- [72] S. G. Rubin, A. S. Sakharov, and M. Y. Khlopov, *J. Exp. Theor. Phys.* **91**, 921 (2001), [arXiv:hep-ph/0106187](#).
- [73] J. Garriga, A. Vilenkin, and J. Zhang, *Journal of Cosmology and Astroparticle Physics* **2016**, 064 (2016).
- [74] S. W. Hawking, *Phys. Lett. B* **231**, 237 (1989).
- [75] A. Polnarev and R. Zembowicz, *Phys. Rev. D* **43**, 1106 (1991).
- [76] J. Garriga and M. Sakellariadou, *Phys. Rev. D* **48**, 2502 (1993), [arXiv:hep-th/9303024](#).
- [77] R. R. Caldwell and P. Casper, *Phys. Rev. D* **53**, 3002 (1996), [arXiv:gr-qc/9509012](#).
- [78] J. H. MacGibbon, R. H. Brandenberger, and U. F. Wichoski, *Phys. Rev. D* **57**, 2158 (1998), [arXiv:astro-ph/9707146](#).
- [79] A. C. Jenkins and M. Sakellariadou, (2020), [arXiv:2006.16249 \[astro-ph.CO\]](#).
- [80] J. Martin, T. Papanikolaou, and V. Vennin, *JCAP* **01**, 024 (2020), [arXiv:1907.04236 \[astro-ph.CO\]](#).
- [81] J. Martin, T. Papanikolaou, L. Pinol, and V. Vennin, *JCAP* **05**, 003 (2020), [arXiv:2002.01820 \[astro-ph.CO\]](#).
- [82] A. M. Green and A. R. Liddle, *Phys. Rev. D* **56**, 6166 (1997), [arXiv:astro-ph/9704251](#).
- [83] T. Bringmann, C. Kiefer, and D. Polarski, *Phys. Rev. D* **65**, 024008 (2002), [arXiv:astro-ph/0109404](#).
- [84] H. I. Kim, C. H. Lee, and J. H. MacGibbon, *Phys. Rev. D* **59**, 063004 (1999), [arXiv:astro-ph/9901030](#).
- [85] B. Carr, M. Raidal, T. Tenkanen, V. Vaskonen, and H. Veermäe, *Phys. Rev. D* **96**, 023514 (2017), [arXiv:1705.05567 \[astro-ph.CO\]](#).
- [86] K. R. Dienes, J. Kumar, P. Stengel, and B. Thomas, *Phys. Rev. D* **99**, 043513 (2019), [arXiv:1810.10587 \[hep-ph\]](#).
- [87] Y. Akrami *et al.* (Planck), *Astron. Astrophys.* **641**, A10 (2020), [arXiv:1807.06211 \[astro-ph.CO\]](#).
- [88] J. H. MacGibbon and B. R. Webber, *Phys. Rev. D* **41**, 3052 (1990).
- [89] J. H. MacGibbon, *Phys. Rev. D* **44**, 376 (1991).
- [90] A. Cheek, L. Heurtier, Y. F. Perez-Gonzalez, and J. Turner, “Friedmann solver for black hole evaporation in the early universe,” <https://github.com/yfperezg/frisbhee>.
- [91] A. H. Guth, *Phys. Rev. D* **23**, 347 (1981).
- [92] A. D. Linde, *Phys. Lett. B* **108**, 389 (1982).
- [93] A. Albrecht and P. J. Steinhardt, *Phys. Rev. Lett.* **48**, 1220 (1982).
- [94] Y. Akrami *et al.* (Planck), *Astron. Astrophys.* **641**, A10 (2020), [arXiv:1807.06211 \[astro-ph.CO\]](#).
- [95] A. R. Liddle and S. M. Leach, *Phys. Rev. D* **68**, 103503 (2003), [arXiv:astro-ph/0305263](#).
- [96] R. Allahverdi, K. Dutta, and A. Maharana, *JCAP* **10**, 038 (2018), [arXiv:1808.02659 \[astro-ph.CO\]](#).
- [97] L. Kofman, A. D. Linde, and A. A. Starobinsky, *Phys. Rev. Lett.* **73**, 3195 (1994), [arXiv:hep-th/9405187](#).
- [98] A. Ghoshal, L. Heurtier, and A. Paul, *JHEP* **12**, 105 (2022), [arXiv:2208.01670 \[hep-ph\]](#).
- [99] L. Heurtier and F. Huang, *Phys. Rev. D* **100**, 043507 (2019), [arXiv:1905.05191 \[hep-ph\]](#).
- [100] R. Kallosh and A. Linde, *JCAP* **07**, 002 (2013), [arXiv:1306.5220 \[hep-th\]](#).
- [101] A. A. Starobinsky, *Phys. Lett. B* **91**, 99 (1980).
- [102] A. A. Starobinsky, *Sov. Astron. Lett.* **9**, 302 (1983).
- [103] P. Ade *et al.* (Simons Observatory), *JCAP* **02**, 056 (2019), [arXiv:1808.07445 \[astro-ph.CO\]](#).
- [104] L. Moncelli *et al.*, *Proc. SPIE Int. Soc. Opt. Eng.* **11453**, 1145314 (2020), [arXiv:2012.04047 \[astro-ph.IM\]](#).
- [105] K. Abazajian *et al.*, (2019), [arXiv:1907.04473 \[astro-ph.IM\]](#).
- [106] T. Opferkuch, P. Schwaller, and B. A. Stefanek, *JCAP* **07**, 016 (2019), [arXiv:1905.06823 \[gr-qc\]](#).
- [107] C. Caprini and D. G. Figueroa, *Class. Quant. Grav.* **35**, 163001 (2018), [arXiv:1801.04268 \[astro-ph.CO\]](#).
- [108] M. Tanabashi *et al.* (Particle Data Group), *Phys. Rev. D* **98**, 030001 (2018).
- [109] P. Amaro-Seoane *et al.* (LISA), (2017), [arXiv:1702.00786 \[astro-ph.IM\]](#).
- [110] J. Baker *et al.*, (2019), [arXiv:1907.06482 \[astro-ph.IM\]](#).
- [111] J. Crowder and N. J. Cornish, *Phys. Rev. D* **72**, 083005 (2005), [arXiv:gr-qc/0506015](#).
- [112] V. Corbin and N. J. Cornish, *Class. Quant. Grav.* **23**, 2435 (2006), [arXiv:gr-qc/0512039](#).
- [113] G. M. Harry, P. Fritschel, D. A. Shaddock, W. Folkner, and E. S. Phinney, *Class. Quant. Grav.* **23**, 4887 (2006), [Erratum: *Class. Quant. Grav.* **23**, 7361 (2006)].
- [114] N. Seto, S. Kawamura, and T. Nakamura, *Phys. Rev. Lett.* **87**, 221103 (2001), [arXiv:astro-ph/0108011](#).
- [115] S. Kawamura *et al.*, *Class. Quant. Grav.* **28**, 094011 (2011).
- [116] K. Yagi and N. Seto, *Phys. Rev. D* **83**, 044011 (2011), [Erratum: *Phys. Rev. D* **95**, 109901 (2017)], [arXiv:1101.3940 \[astro-ph.CO\]](#).
- [117] H. Kudoh, A. Taruya, T. Hiramatsu, and Y. Himemoto, *Phys. Rev. D* **73**, 064006 (2006), [arXiv:gr-qc/0511145](#).
- [118] K. Saikawa and S. Shirai, *JCAP* **05**, 035 (2018), [arXiv:1803.01038 \[hep-ph\]](#).
- [119] A. Ringwald, K. Saikawa, and C. Tamarit, *JCAP* **02**, 046 (2021), [arXiv:2009.02050 \[hep-ph\]](#).
- [120] J. Garcia-Bellido, H. Murayama, and G. White, *JCAP* **12**, 023 (2021), [arXiv:2104.04778 \[hep-ph\]](#).
- [121] A. Sesana *et al.*, *Exper. Astron.* **51**, 1333 (2021), [arXiv:1908.11391 \[astro-ph.IM\]](#).
- [122] G. M. Harry (LIGO Scientific), *Class. Quant. Grav.* **27**, 084006 (2010).
- [123] J. Aasi *et al.* (LIGO Scientific), *Class. Quant. Grav.* **32**, 074001 (2015), [arXiv:1411.4547 \[gr-qc\]](#).

- [124] F. Acernese *et al.* (VIRGO), *Class. Quant. Grav.* **32**, 024001 (2015), arXiv:1408.3978 [gr-qc].
- [125] R. Abbott *et al.* (LIGO Scientific, Virgo), *SoftwareX* **13**, 100658 (2021), arXiv:1912.11716 [gr-qc].
- [126] B. P. Abbott *et al.* (LIGO Scientific), *Class. Quant. Grav.* **34**, 044001 (2017), arXiv:1607.08697 [astro-ph.IM].
- [127] D. Reitze *et al.*, *Bull. Am. Astron. Soc.* **51**, 035 (2019), arXiv:1907.04833 [astro-ph.IM].
- [128] S. Hild *et al.*, *Class. Quant. Grav.* **28**, 094013 (2011), arXiv:1012.0908 [gr-qc].
- [129] M. Maggiore *et al.*, *JCAP* **03**, 050 (2020), arXiv:1912.02622 [astro-ph.CO].
- [130] S. Matarrese, O. Pantano, and D. Saez, *Phys. Rev. D* **47**, 1311 (1993).
- [131] S. Matarrese, O. Pantano, and D. Saez, *Phys. Rev. Lett.* **72**, 320 (1994), arXiv:astro-ph/9310036.
- [132] S. Matarrese, S. Mollerach, and M. Bruni, *Phys. Rev. D* **58**, 043504 (1998), arXiv:astro-ph/9707278.
- [133] H. Noh and J.-c. Hwang, *Phys. Rev. D* **69**, 104011 (2004).
- [134] C. Carbone and S. Matarrese, *Phys. Rev. D* **71**, 043508 (2005), arXiv:astro-ph/0407611.
- [135] K. Nakamura, *Prog. Theor. Phys.* **117**, 17 (2007), arXiv:gr-qc/0605108.
- [136] D. Baumann, P. J. Steinhardt, K. Takahashi, and K. Ichiki, *Phys. Rev. D* **76**, 084019 (2007), arXiv:hep-th/0703290.
- [137] T. Nakama, J. Silk, and M. Kamionkowski, *Phys. Rev. D* **95**, 043511 (2017), arXiv:1612.06264 [astro-ph.CO].
- [138] G. Domènech, *Int. J. Mod. Phys. D* **29**, 2050028 (2020), arXiv:1912.05583 [gr-qc].
- [139] K. Inomata, M. Kawasaki, K. Mukaida, T. Terada, and T. T. Yanagida, *Phys. Rev. D* **101**, 123533 (2020), arXiv:2003.10455 [astro-ph.CO].
- [140] K. Inomata, K. Kohri, T. Nakama, and T. Terada, *Phys. Rev. D* **100**, 043532 (2019), arXiv:1904.12879 [astro-ph.CO].
- [141] K. Inomata, K. Kohri, T. Nakama, and T. Terada, *JCAP* **10**, 071 (2019), arXiv:1904.12878 [astro-ph.CO].
- [142] A. Ito, T. Ikeda, K. Miuchi, and J. Soda, *Eur. Phys. J. C* **80**, 179 (2020), arXiv:1903.04843 [gr-qc].
- [143] A. Ejlli, D. Ejlli, A. M. Cruise, G. Pisano, and H. Grote, *Eur. Phys. J. C* **79**, 1032 (2019), arXiv:1908.00232 [gr-qc].
- [144] A. Berlin, D. Blas, R. Tito D'Agnolo, S. A. R. Ellis, R. Harnik, Y. Kahn, and J. Schütte-Engel, *Phys. Rev. D* **105**, 116011 (2022), arXiv:2112.11465 [hep-ph].
- [145] V. Domcke, C. Garcia-Cely, and N. L. Rodd, *Phys. Rev. Lett.* **129**, 041101 (2022), arXiv:2202.00695 [hep-ph].
- [146] A. Ito and J. Soda, (2022), arXiv:2212.04094 [gr-qc].
- [147] D. Inman and Y. Ali-Haïmoud, *Phys. Rev. D* **100**, 083528 (2019), arXiv:1907.08129 [astro-ph.CO].
- [148] H. Kodama and M. Sasaki, *Int. J. Mod. Phys. A* **1**, 265 (1986).
- [149] H. Kodama and M. Sasaki, *Int. J. Mod. Phys. A* **2**, 491 (1987).
- [150] T. Papanikolaou, V. Venmin, and D. Langlois, *JCAP* **03**, 053 (2021), arXiv:2010.11573 [astro-ph.CO].
- [151] G. Domènech, C. Lin, and M. Sasaki, *JCAP* **04**, 062 (2021), [Erratum: *JCAP* **11**, E01 (2021)], arXiv:2012.08151 [gr-qc].
- [152] J. Kozaczuk, T. Lin, and E. Villarama, *Phys. Rev. D* **105**, 123023 (2022), arXiv:2108.12475 [astro-ph.CO].
- [153] T. Papanikolaou, C. Tzerefos, S. Basilakos, and E. N. Saridakis, *JCAP* **10**, 013 (2022), arXiv:2112.15059 [astro-ph.CO].
- [154] N. Bhaumik, A. Ghoshal, and M. Lewicki, *JHEP* **07**, 130 (2022), arXiv:2205.06260 [astro-ph.CO].
- [155] N. Bhaumik, A. Ghoshal, R. K. Jain, and M. Lewicki, (2022), arXiv:2212.00775 [astro-ph.CO].
- [156] T. Papanikolaou, C. Tzerefos, S. Basilakos, and E. N. Saridakis, *Eur. Phys. J. C* **83**, 31 (2023), arXiv:2205.06094 [gr-qc].
- [157] T. Papanikolaou, *JCAP* **10**, 089 (2022), arXiv:2207.11041 [astro-ph.CO].
- [158] J. Auffinger, (2022), arXiv:2206.02672 [astro-ph.CO].
- [159] D. N. Page, *Phys. Rev. D* **13**, 198 (1976).
- [160] D. N. Page, *Phys. Rev. D* **14**, 3260 (1976).
- [161] D. N. Page, *Phys. Rev. D* **16**, 2402 (1977).
- [162] D. Hooper, G. Krnjaic, J. March-Russell, S. D. McDermott, and R. Petrossian-Byrne, (2020), arXiv:2004.00618 [astro-ph.CO].
- [163] A. Cheek, L. Heurtier, Y. F. Perez-Gonzalez, and J. Turner, (2022), arXiv:2212.03878 [hep-ph].
- [164] K. N. Abazajian *et al.* (CMB-S4), (2016), arXiv:1610.02743 [astro-ph.CO].
- [165] S. Aiola *et al.* (CMB-HD), (2022), arXiv:2203.05728 [astro-ph.CO].
- [166] G. E. A. Matsas, J. C. Montero, V. Pleitez, and D. A. T. Vanzella, in *Conference on Topics in Theoretical Physics II: Festschrift for A.H. Zimerman* (1998) arXiv:hep-ph/9810456.
- [167] N. F. Bell and R. R. Volkas, *Phys. Rev. D* **59**, 107301 (1999), arXiv:astro-ph/9812301 [astro-ph].
- [168] T. Fujita, M. Kawasaki, K. Harigaya, and R. Matsuda, *Phys. Rev. D* **89**, 103501 (2014), arXiv:1401.1909 [astro-ph.CO].
- [169] P. McDonald *et al.* (SDSS), *Astrophys. J. Suppl.* **163**, 80 (2006), arXiv:astro-ph/0405013.
- [170] G. D. Becker, M. Rauch, and W. L. W. Sargent, *Astrophys. J.* **662**, 72 (2007), arXiv:astro-ph/0607633.
- [171] G. D. Becker, J. S. Bolton, M. G. Haehnelt, and W. L. W. Sargent, *Mon. Not. Roy. Astron. Soc.* **410**, 1096 (2011), arXiv:1008.2622 [astro-ph.CO].
- [172] A. P. Calverley, G. D. Becker, M. G. Haehnelt, and J. S. Bolton, *Mon. Not. Roy. Astron. Soc.* **412**, 2543 (2011), arXiv:1011.5850 [astro-ph.CO].
- [173] G. D. Becker, W. L. W. Sargent, M. Rauch, and A. P. Calverley, *Astrophys. J.* **735**, 93 (2011), arXiv:1101.4399 [astro-ph.CO].
- [174] C. P. Ahn *et al.* (SDSS), *Astrophys. J. Suppl.* **211**, 17 (2014), arXiv:1307.7735 [astro-ph.IM].
- [175] S. López *et al.*, *Astron. Astrophys.* **594**, A91 (2016), arXiv:1607.08776 [astro-ph.GA].
- [176] K. R. Dienes and B. Thomas, *Phys. Rev. D* **85**, 083523 (2012), arXiv:1106.4546 [hep-ph].
- [177] K. R. Dienes and B. Thomas, *Phys. Rev. D* **85**, 083524 (2012), arXiv:1107.0721 [hep-ph].
- [178] K. R. Dienes and B. Thomas, *Phys. Rev. D* **86**, 055013 (2012), arXiv:1203.1923 [hep-ph].
- [179] M. Joyce, *Phys. Rev. D* **55**, 1875 (1997), arXiv:hep-ph/9606223.
- [180] M. Joyce and T. Prokopec, *Phys. Rev. D* **57**, 6022 (1998), arXiv:hep-ph/9709320.
- [181] G. Servant, *JHEP* **01**, 044 (2002), arXiv:hep-ph/0112209.



- [182] G. Barenboim and J. Rasero, *JHEP* **07**, 028 (2012), [arXiv:1202.6070 \[hep-ph\]](#).
- [183] D. Toussaint, S. B. Treiman, F. Wilczek, and A. Zee, *Phys. Rev. D* **19**, 1036 (1979).
- [184] M. S. Turner, *Phys. Lett. B* **89**, 155 (1979).
- [185] A. F. Grillo, *Phys. Lett. B* **94**, 364 (1980).
- [186] A. Hook, *Phys. Rev. D* **90**, 083535 (2014), [arXiv:1404.0113 \[hep-ph\]](#).
- [187] A. Granelli, K. Moffat, Y. F. Perez-Gonzalez, H. Schulz, and J. Turner, *Comput. Phys. Commun.* **262**, 107813 (2021), [arXiv:2007.09150 \[hep-ph\]](#).
- [188] A. Chaudhuri and A. Dolgov, (2020), [arXiv:2001.11219 \[astro-ph.CO\]](#).
- [189] N. Bernal, C. S. Fong, Y. F. Perez-Gonzalez, and J. Turner, *Phys. Rev. D* **106**, 035019 (2022), [arXiv:2203.08823 \[hep-ph\]](#).
- [190] A. L. Erickcek and K. Sigurdson, *Phys. Rev. D* **84**, 083503 (2011), [arXiv:1106.0536 \[astro-ph.CO\]](#).
- [191] J. Fan, O. Özsoy, and S. Watson, *Phys. Rev. D* **90**, 043536 (2014), [arXiv:1405.7373 \[hep-ph\]](#).
- [192] J. Georg, G. Şengör, and S. Watson, *Phys. Rev. D* **93**, 123523 (2016), [arXiv:1603.00023 \[hep-ph\]](#).